NASA TECHNICAL NOTE

NASA TN D-2659

NASA TN D-2659

ELECTRON-BREMSSTRAHLUNG DIFFERENTIAL CROSS SECTIONS FOR THIN AND THICK TARGETS

by W. Wayne Scott

Langley Research Center

Langley Station, Hampton, Va.

NATIONAL AERONAUTICS AND SPACE ADMINISTRATION • WASHINGTON, D. C. • MARCH 1965

NASA TN D-2659

ELECTRON-BREMSSTRAHLUNG DIFFERENTIAL CROSS SECTIONS FOR THIN AND THICK TARGETS

By W. Wayne Scott

Langley Research Center
Langley Station, Hampton, Va.

NATIONAL AERONAUTICS AND SPACE ADMINISTRATION

For sale by the Office of Technical Services, Department of Commerce,
Washington, D.C. 20230 - Price $3.00

ELECTRON-BREMSSTRAHLUNG DIFFERENTIAL CROSS SECTIONS FOR THIN AND THICK TARGETS

By W. Wayne Scott
Langley Research Center

SUMMARY

Thin- and thick-target bremsstrahlung spectra are presented for electron energies up to 7.0 MeV. The thin-target results were determined from bremsstrahlung differential cross-section relations, whereas the thick-target spectra were evaluated by assuming that the total emission spectrum from a thick target is a summation over each of the spectra from a series of thin targets, one behind the other, with the energy of the incident electron decreasing for each succeeding thin target. Photon attenuation within the target has been considered. The computational procedure for computing the thin-target relations has been programed in the FORTRAN (FORmula TRANslation) II language for the IBM 7094 electronic data processing system and is presented in appendixes.

INTRODUCTION

The electrons that exist in the radiation belt surrounding the earth present a radiation hazard to man and equipment in space explorations. This hazard has been intensified by the creation of the artificial electron belt by the recent nuclear explosions in space. (See, for example, ref. 1.) The hazard to space vehicles from electrons exists primarily in the form of a penetrating secondary radiation that is produced by the energy degradation of the electrons within the space-vehicle wall. This radiation, designated as bremsstrahlung, results from a direct interaction of incoming electrons with the coulomb fields of the nuclei of the elements which comprise the space-vehicle wall.

A vehicle wall can be treated as a thin target if, while traversing the wall, the incident electron has only one radiative collision, suffers no significant elastic deflection, and loses no appreciable energy by ionization. However, this wall thickness is seldom the case. Generally, a space-vehicle wall will be of such thickness that the majority of the incident electrons will lose sufficient energy to be stopped. For this case, the description of the bremsstrahlung field is greatly complicated by the fact that the electron encounters many scattering centers and is continually losing energy in a random manner. Such calculations are necessarily complicated, and no exact analytical expression exists for the determination of thick-target bremmstrahlung spectra. In this paper a method is presented for determining thick-target spectra by utilizing thin-target cross-section data. The angular scattering of the electron

within the target itself has not been considered in determining the thick-target spectra. The thin-target differential cross sections utilized in the calculation are based on Bethe-Heitler theory, as given by the relations in reference 2, and are presented in graphical form for incident-electron energies ranging from 0.1 to 7.0 MeV. In addition, the thin-target computational procedure as programed for the IBM 7094 computer is presented in the appendixes.

SYMBOLS

c	speed of light, cm/sec
E	final total energy of electron in a collision, $T + 1$, in units of $m_o c^2$
E_i	total energy of electron emergent from thin target i ($i = 1, 2, \ldots n$), in units of $m_o c^2$
E_o	initial total energy of electron in a collision, $T_o + 1$, in units of $m_o c^2$
E_t	total electron energy, in units of $m_o c^2$
ΔE	increment in electron energy, in units of $m_o c^2$
e	electron charge, esu
h	Planck's constant, erg/sec
$\hbar = \frac{h}{2\pi}$, erg/sec	
I	intensity of emitted photons
$\overline{I}$	mean ionization potential, in units of $m_o c^2$
i	index integer
K	semiempirical constant, $\left(m_o c^2\right)^{-1}$
k	vector energy of emitted photon, in units of $m_o c^2$
m_o	electron rest mass, grams
$m_o c^2$	electron rest-mass energy, 0.511 MeV
N	atomic density of target material, atoms/cm^3

N_a	number of atoms per centimeter for a unit area
n	number of thick-target subdivisions
p	final momentum vector of electron after collision, $\left[T(T + 2)\right]^{1/2}$, in units of $m_o c$
p_o	initial momentum vector of electron prior to collision, $\left[T_o(T_o + 2)\right]^{1/2}$, in units of $m_o c$
r_o	classical electron radius, cm
ds	increment of electron path length
T	final kinetic energy of electron in a collision, in units of $m_o c^2$
T_o	initial kinetic energy of electron in a collision, in units of $m_o c^2$
t	line-of-sight distance in target material between source point of photon and target exit position, cm
v	velocity of electron after collision, cm/sec
v_i	velocity of incident electron, cm/sec
v_o	velocity of electron before collision, cm/sec
X_t, Y_t, Z_t	coordinate axes of target
$\bar{X}$	average target thickness, cm
ΔX_i	increment of target thickness, cm
x,y	coordinates along X_t- and Y_t-axes, respectively
Z	atomic charge number of target material
β	ratio of electron speed in collision to speed of light, $\frac{v_i}{c}$
θ	angle of k with respect to p, deg
θ_o	photon emission angle of k with respect to p_o, deg
$\mu(k)$	photon-attenuation coefficient as function of photon energy k and target element, cm^{-1}

$d\sigma$	differential bremsstrahlung cross section, cm^2/atom-electron
φ	polar angle referred to k
Ω_k	solid angle, sr
$d\Omega_k$	element of solid angle in k direction, $\sin \theta_o \, d\theta_o \, d\varphi$, sr

THIN-TARGET ANALYSIS

Born Approximation Cross-Section Formulas

In quantum-mechanical theory an electron can be represented by a plane wave. (See, for example, ref. 3.) Upon entering the nuclear coulomb field, this wave is scattered and has a small but finite chance of emitting a photon as a result of the interaction of the plane wave with the coulomb field of the nucleus. In a radiative collision of this kind, the initial momentum of the incident electron becomes shared among the momenta of three bodies: the scattered electron, the atomic nucleus, and the emitted photon. Therefore, the photon can have any momentum up to the momentum of the incident electron. For the radiative collision of moderate-energy electrons, momentum is essentially conserved between the nucleus and the deflected electron. Only a very small momentum is carried away by the photon, and it can be emitted in any direction. At extreme relativistic energies, however, both the photon and the scattered electron tend to proceed in the same direction as the incident electron.

The quantum-mechanical theory for thin-target bremsstrahlung has been developed by Bethe and Heitler and by Sauter (ref. 2) and uses the Born approximation technique, which is essentially first-order pertubation theory. In general, the reliability of the Born approximation technique decreases with increasing atomic number of the target material and gives correct results only if

$$\frac{2\pi Ze^2}{\hbar v_o} \ll 1 \tag{1}$$

and

$$\frac{2\pi Ze^2}{\hbar v} \ll 1 \tag{2}$$

where v_o and v represent the velocity of the electron before and after the collision, respectively. The Born approximation cross-section formulas have been successful in predicting the properties of bremsstrahlung radiation in spite of the limiting restrictions given by equations (1) and (2). Even when there is a violation of these restrictions, the cross-section formulas can be expected to give at least the correct order of magnitude, except at the high

frequency limit - that is, where the photon energy approaches the initial electron energy.

The Born approximation cross-section formulas can be expressed in various differential forms; for example, the cross sections (radiative probabilities) can be expressed as differentials with respect to two parameters, the photon energy k and the solid angle Ω_k, as shown by the following equation. (See formula 2BN of ref. 2.)

$$d\sigma(k,\theta_o,\varphi) = \frac{Z^2 r_o^2}{8\pi 137}\frac{p}{p_o}\frac{dk}{k}d\Omega_k\left\{\frac{8\left(2E_o^2+1\right)\sin^2\theta_o}{p_o^2\Delta_o^4} - \frac{2\left(5E_o^2+2EE_o+3\right)}{p_o^2\Delta_o^3}\right.$$

$$- \frac{2\left(p_o^2-k^2\right)}{Q^2\Delta_o^2} + \frac{4E}{p_o^2\Delta_o} + \frac{L}{pp_o}\left[\frac{4E_o\left(3k-p_o^2E\right)\sin^2\theta_o}{p_o^2\Delta_o^4}\right.$$

$$+ \frac{4E_o^2\left(E_o^2+E^2\right)}{p_o^2\Delta_o^2} + \frac{2-2\left(7E_o^2-3EE_o+E^2\right)}{p_o^2\Delta_o^2}$$

$$\left.\left.+ \frac{2k\left(E_o^2+EE_o-1\right)}{p_o^2\Delta_o}\right] - \frac{4\epsilon}{p\Delta_o} + \frac{\epsilon Q}{pQ}\left[\frac{4}{\Delta_o^2} - \frac{6k}{\Delta_o} - \frac{2k\left(p_o^2-k^2\right)}{Q^2\Delta_o}\right]\right\} \quad (3)$$

where

$$L = \log_e\left[\frac{EE_o - 1 + pp_o}{EE_o - 1 - pp_o}\right]$$

$$Q^2 = p_o^2 + k^2 - 2p_o k\cos\theta_o$$

$$\Delta_o = E_o - p_o\cos\theta_o$$

$$\epsilon = \log_e\left[\frac{E+p}{E-p}\right]$$

and

$$\epsilon^{Q} = \log_e\left[\frac{Q + p}{Q - p}\right]$$

Equation (3) represents the probability that a photon whose energy lies between the limits k and $k + dk$ shall be emitted within a differential solid angle $d\Omega_k$, orientated at some angle θ_o with respect to the direction of motion of the incident electron when an electron of total energy E_o collides with a thin target of atomic number Z. This collision geometry is shown in figure 1 for an electron approaching the origin along the negative Z_t-axis with momentum p_o and colliding with a thin target, which is considered to lie in the xy-plane, perpendicular to the electron direction.

The probability of photon emission integrated over all angles θ_o and φ is shown by the following equation. (See formula 3BN of ref. 2.)

$$d\sigma(k) = \frac{Z^2 r_o^2}{137}\frac{p}{p_o}\frac{dk}{k}\left(\frac{4}{3} - 2EE_o\left(\frac{p^2 + p_o^2}{p^2 p_o^2}\right) + \frac{\epsilon_o E}{p_o^3} + \frac{\epsilon E_o}{p^3} - \frac{\epsilon\epsilon_o}{pp_o} + L_1\left\{\frac{8EE_o}{3pp_o}\right.\right.$$

$$\left. + \frac{k^2\left(E^2E_o^2 + p^2p_o^2\right)}{p^3p_o^3} + \frac{k}{2pp_o}\left[\left(\frac{EE_o + p_o^2}{p_o^3}\right)\epsilon_o - \left(\frac{EE_o + p^2}{p^3}\right)\epsilon\right.\right.$$

$$\left.\left. + \frac{2kEE_o}{p^2p_o^2}\right]\right\}\Bigg) \qquad (4)$$

where

$$L_1 = 2\log_e\left[\frac{EE_o - 1 + pp_o}{k}\right]$$

$$\epsilon = \log_e\left(\frac{E + p}{E - p}\right)$$

and

$$\epsilon_o = \log_e\left(\frac{E_o + p_o}{E_o - p_o}\right)$$

Solutions to equations (3) and (4) were readily obtained with the aid of a high-speed electronic digital computer. Descriptions of the FORTRAN II computer programs and the program listings are presented in the appendixes.

Graphical Representation of the Thin-Target Formulas

The dependence of the thin-target cross section on the electron and photon energies and the photon emission angle is presented in figures 2 to 6. Equation (3) has been evaluated for electron energies from 0.1 to 7.0 MeV and for angles of 0°, 30°, 60°, and 90° with respect to the incident-electron direction. The results of this evaluation are shown in figure 2 in which the ordinate is a quantity defined as intensity $\left(\text{photon energy } k \text{ times the number of photons } \frac{d\sigma}{dk\, d\Omega_k} \text{ with energy } k\right)$. For convenience the curves have been made independent of the atomic number Z, and the cross section is for a unit monoenergetic electron flux. The figures show that for electron kinetic energies of the order of or greater than the electron rest-mass energy (0.511 MeV), the differential cross section decreases with increasing emission angle θ_o. However, for electron kinetic energies that are small compared with the electron rest-mass energy, the cross section becomes a maximum at right angles with respect to the incident-electron direction.

Figure 3 shows the dependence of the bremsstrahlung-spectrum shape on the incident-electron energy as obtained by evaluating equation (4). Again the ordinate is a quantity defined as intensity $\left(\text{photon energy } k \text{ times the number of photons } \frac{d\sigma}{dk} \text{ with energy } k\right)$. Results for several electron kinetic energies are plotted on each graph. The cross section is seen to decrease with increasing photon energy for each electron kinetic energy.

Some indications of the limitations of the Born approximation can be seen by comparison of the theoretical cross sections with experimental data. For electron kinetic energies of the same order of magnitude as the electron rest-mass energy, the Born approximation theory underestimates the experimental cross sections, as shown in figures 4 and 5, which are taken from reference 2. However, for electron kinetic energies that are large compared with the electron rest-mass energy, the experimental results shown in figure 6 (taken from ref. 4) agree within 10 percent with the Born approximation theory.

THICK-TARGET ANALYSIS

The previous thin-target relations (eqs. (3) and (4)) and results are for a single scattering only; that is, the path length within the target is taken to be small enough that the probability of a scattering is very small. The probability that the same electron will be scattered twice in this distance is then negligible. When thicker layers of absorbing material are considered, the incident electron encounters many scattering centers. This multiple encounter of nuclei results in a random path for each electron within the target and, as a result, the angular distribution of the bremsstrahlung is affected. The thick-target bremsstrahlung cross sections could conceivably be obtained by utilizing electron scattering analyses in which the path of the electron is traced through the target, and the direction of photon emission is related to the electron direction at each scatter. Such an analysis is complex, and even on a high-speed digital computer it is time consuming to perform. A simplified approach is presented to approximate the thick-target bremsstrahlung spectra; this approach is made on the assumption that the total emission spectrum from a thick target is a summation over each of the spectra from a series of thin targets, one behind the other, with the energy of the incident electron decreasing for each succeeding thin target. Also, the following assumptions have been made:

(a) The electron loses energy along a straight-line path within the target and has a range equal to the mean-path length.

(b) The intensity spectra will be considered without regard to the angular distribution, and the total intensity is the intensity integrated over all angles θ_o and φ.

Assumption (a) is justifiable in that the electron-scattering cross-section curve is peaked in the forward direction for energies greater than approximately 0.5 MeV. For example, in the stopping of 1-MeV electrons in a thick carbon target, the majority of the electrons are contained within a cone of half-angle equal to approximately 10°.

Assumption (b) is justifiable in that it is more probable that the photons are emitted in the forward direction for electrons with energies greater than approximately 0.1 MeV, and with increasing electron energies this peaking becomes more pronounced.

In this analysis, a thick target is defined as one whose thickness is equal to the mean range of the incident electron, as given by ionization energy-loss relations.

Electron Energy-Loss Mechanism in Target

The energy loss of electrons in a medium essentially occurs by two different mechanisms. The predominant mechanism of energy degradation at lower energies is due to the inelastic collisions with the electrons of the medium,

whereas at higher energies radiative collisions with the electric fields of the nuclei and electrons become more important. It is shown on page 610 of reference 5 that for lead the electron energy loss per unit path length of travel due to ionization is equal to that for radiative collisions at an approximate electron energy of 9 MeV, whereas for materials with lower atomic numbers the equality occurs at much higher energies. For the calculations presented, it is assumed that the initial energy of the electron is sufficiently small so that the energy loss as a result of radiative collisions is negligible in comparison with the loss resulting from inelastic collisions.

The energy loss per centimeter path length due to ionizing collisions of the electron is (see p. 254 of ref. 6):

$$-\frac{dE_t}{ds} = \frac{2\pi N e^4 Z}{m_o v_i^2}\left[\log_e \frac{m_o v_i^2 E_t}{2\bar{I}^2\left(1-\beta^2\right)} - \left(2\sqrt{1-\beta^2} - 1 + \beta^2\right)\log_e 2 + 1 - \beta^2 + \frac{1}{8}\left(1-\sqrt{1-\beta^2}\right)^2\right] \tag{5}$$

As shown by equation (5), the energy loss per path increment is nonlinear with respect to the electron energy, and the electron loses energy at an increasing rate as it slows down.

Development of Thick-Target Relations

Sketch (a) shows a thick target subdivided into a series of thin targets.

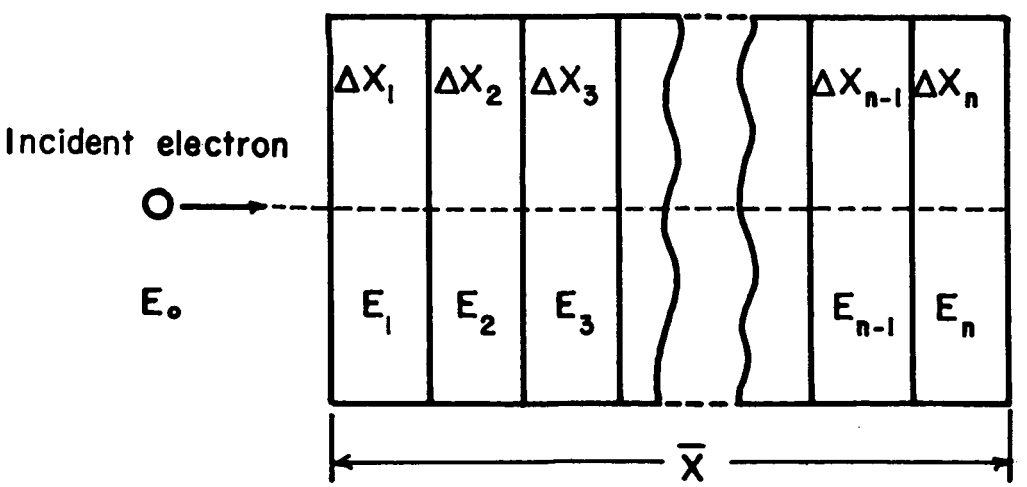

Sketch (a)

The bremsstrahlung differential cross section for a unit area with an incremental thickness ΔX_i and with a corresponding electron energy E_i will be taken to be that for a section 1 atom thick times the number of atoms per unit length. Thus,

$$\left(\frac{k}{Z^2}\frac{d\sigma}{dk}\right)_i = \left(\frac{k}{Z^2}\frac{d\sigma}{dk}\right)\Delta X_i N_a \tag{6}$$

where N_a is the number of atoms per centimeter for a unit area. If the energy loss is considered to be linear through the target, then the total number of increments n is given by

$$n = \frac{\bar{X}}{\Delta X} = \frac{E_o}{\Delta E} \tag{7}$$

where E_o is the initial total incident electron energy and $\bar{X}$ is the target thickness, or the range of an electron with energy E_o, when it is assumed that ionization is the only energy-loss mechanism.

With the use of equation (7), equation (6) may be written as

$$\left(\frac{k}{Z^2}\frac{d\sigma}{dk}\right)_i = \left(\frac{k}{Z^2}\frac{d\sigma}{dk}\right)\frac{\bar{X}}{n} N_a \tag{8}$$

and the total differential cross section for the composite thick target is

$$\left(\frac{k}{Z^2}\frac{d\sigma}{dk}\right)_{thick} = \frac{N_a\bar{X}}{n}\sum_{i=1}^{n}\left(\frac{k}{Z^2}\frac{d\sigma}{dk}\right)_i \tag{9}$$

where $\left(\frac{k}{Z^2}\frac{d\sigma}{dk}\right)_i$ is evaluated for the energy in the corresponding target-thickness increment ΔX_i.

Equation (9) lends itself easily to hand calculations with the use of the cross-section results shown in figure 3. The result of such a calculation is

presented in figure 7 for an electron with a kinetic energy of 1 MeV which is stopped in a thick target of carbon.

As previously stated, the energy loss per centimeter path length is not linear with respect to the electron energy, and a more refined approximation than the one given by equation (9) would account for this nonlinearity. In theory it is possible to determine the differential path length of an electron within an absorber with the use of equation (5), the relation expressing energy loss per centimeter path length. The differential path length is expressed as

$$ds = \frac{dE}{-\frac{dE}{ds}} \tag{10}$$

or

$$\Delta X = \frac{\Delta E}{-\frac{\Delta E}{\Delta X}} \tag{11}$$

Thus, the nonlinearity can be accounted for by the substitution of equation (11) into equation (6), yielding:

$$\left(\frac{k}{Z^2}\frac{d\sigma}{dk}\right)_i = \left(\frac{k}{Z^2}\frac{d\sigma}{dk}\right)_i \frac{\Delta E}{-\frac{\Delta E}{\Delta X}} N_a \tag{12}$$

The thick-target differential cross section may then be written as

$$\left(\frac{k}{Z^2}\frac{d\sigma}{dk}\right)_{thick} = N_a \sum_{i=1}^{n} \left(\frac{k}{Z^2}\frac{d\sigma}{dk}\right)_i \frac{\Delta E}{-\frac{\Delta E}{\Delta X}} \tag{13}$$

Equation (13) can be expressed in integral form for an electron of total energy E_o and for a photon of energy k as

$$I(E_o,k) \equiv k\frac{d\sigma}{dk} = N_a Z^2 \int_{k+1}^{E_o} \frac{k}{Z^2}\frac{d\sigma}{dk}\frac{dE}{-\frac{dE}{ds}} \tag{14}$$

where $I(E_o,k)$ is the intensity of the emitted photons per unit photon energy per electron.

Typical curves of bremsstrahlung spectra applicable to all atomic numbers Z can not be drawn as was done for the thin target because the energy loss $-\frac{dE}{ds}$ is a function of Z.

It is now desired to account for the photon attenuation within the target. By previous definition, a thick target is one that stops the electrons incident upon it and for which the target thickness corresponds to the mean path length of an electron with total energy E_o in a material of particular Z. Thus, there will exist some distance through which the photons must travel within the target after their creation. Through this distance, attenuation and absorption of the photons may take place. To account for the photon attenuation it is necessary to know the point of generation of the photon and the distance that it must travel to exit from the target. This distance corresponds to the residual range of the electron at that particular point of photon generation. Thus, the intensity spectrum with photon attenuation within the target is

$$I(E_o,k) = N_a Z^2 \int_{k+1}^{E_o} \left(\frac{k}{Z^2}\frac{d\sigma}{dk}\right) \frac{e^{-\mu(k)t}}{-\frac{dE}{ds}}\, dE \qquad (15)$$

The results obtained by applying the thick-target relations to specific target elements are presented in figures 7 to 12. These results were obtained by numerical integration of equation (15). In figure 7 a comparison is shown between the results obtained by using the thick-target relation when a linear electron energy loss (eq. (9)) and a nonlinear electron energy loss (eq. (15)) are assumed. The difference between the two curves presented results primarily because of the assumption made on the mode of energy loss. If photon attenuation within the target were not considered, it would increase the lower curve by only about 5 percent.

The intensity spectra for thick carbon, aluminum, silicon, and iron targets are presented in figure 8. For convenience, several different electron kinetic energies are plotted on each graph for each material. The ordinate represents the bremsstrahlung intensity and, as to be expected, the intensity is seen to increase with increasing electron energy.

A comparison of the dependence of the thick-target bremsstrahlung spectra on the atomic number Z is shown in figure 9 for carbon (Z = 6), aluminum (Z = 13), silicon (Z = 14), and iron (Z = 26) for an electron with a kinetic energy of 2 MeV. Photon attenuation is greatest for the low-energy photons and is seen to increase with increasing atomic number. This condition is very apparent for the thick iron target for the low-energy photons. The bremsstrahlung intensity spectra also show a strong dependence on the atomic number Z.

A scarcity of experimental thick-target results prevents a complete comparison between theory and experiment over a wide range of electron energies and

atomic numbers. Experimental data[1] for 1.0-MeV electrons stopped in a thick aluminum target are compared with the theoretical data from the present analysis, as shown in figure 10. The theory is seen to compare favorably with the experimental data over the range of photon energy. The discrepancy that exists as photon energy increases is presumed to be due the use of the Born approximation technique in the theoretical model.

The total bremsstrahlung energy created for an electron of initial kinetic energy T_o which is stopped in a thick target can be determined from the results presented within this report (fig. 8) by determining the area under the corresponding curve. This energy intensity may be expressed as

$$I(E_o) = N_a Z^2 \int_{0.05}^{E_o - 1} \int_{k+1}^{E_o} \left(\frac{k}{Z^2} \frac{d\sigma}{dk}\right) \frac{e^{-\mu(k)t}}{-\frac{dE}{ds}} \, dE \, dk \tag{16}$$

where $I(E_o)$ represents the total bremsstrahlung energy created when an electron of total energy E_o is stopped in a thick target. Results obtained by numerical integration of equation (16) for carbon ($Z = 6$) are shown in figure 11 and are compared with results obtained from a semiempirical relationship given by

$$I(E_o) = KZE_o^2 \tag{17}$$

where K is an experimentally determined constant. The value of K used in this comparison is 0.2044×10^{-3}, as can be derived from the value given on page 616 of reference 5. The agreement between the results predicted by this analysis (eq. (16)) and the semiempirically predicted results (eq. (17)) indicates that the previous assumptions (a) and (b) are reasonably valid.

The difference between the two curves may be due in part to the lower limit of the photon energy in equation (16) having been chosen arbitrarily to be 0.05 instead of zero. It is necessary to choose some value other than zero because the differential cross section is undefined for k equal to zero.

A comparison between the total bremsstrahlung energy as a function of the atomic number Z for a 2.0-MeV electron is presented in figure 12. Here again the theoretical and semiempirical results compare favorably. These results show the best comparisons for materials of intermediate Z (silicon and aluminum), a fact which is inherent of the Born approximation.

---

[1]Data from paper (sponsored by NASA Headquarters under Contract No. NASw-647) by L. L. Baggerly, W. E. Dance, B. J. Farmer, and J. H. Johnson of Ling-Temco-Vought Research Center, Nuclear Science Group, Dallas, Texas, presented at Second Symposium on Protection Against Radiation in Space, Gatlinburg, Tennessee, Oct. 12-14, 1964.

Restrictions on Born Approximation

The Born approximation technique applies to elements with intermediate values of Z, and therefore the thick-target relations derived herein are most applicable within this range. For the thick-target relations, the electron energy should be restricted below the point where the electron energy loss as a result of radiative collisions equals the energy loss for inelastic collisions. The use of the thin-target Born approximation cross-section relation for deriving the thick-target expressions introduces two errors that are unavoidable. The thin-target Born approximation cross section is slightly in error at the high frequency limit where the photon energy approaches the incident-electron energy. The other error is introduced because the cross-section relation does not include electron screening.

CONCLUDING REMARKS

Electron-bremsstrahlung differential cross sections, based on the Born approximation, have been computed for thin and thick targets. The thin-target results have been used to predict the bremsstrahlung cross sections for targets with a thickness equal to the mean range of the incident electron. The analysis shows that the assumption of linear energy loss of the electron in the target leads to estimates of bremsstrahlung spectra which are considerably higher than those obtained by considering nonlinear ionization energy loss.

The total bremsstrahlung energy as given by the thick-target analysis agrees favorably with a semiempirical relationship based on experimental data. Comparison of the computed thick-target spectra with experimental measurements shows favorable agreement over most of the photon-energy range but underestimates the measurements at the higher photon energies. This discrepancy with increasing photon energy is expected, inasmuch as the Born approximation technique is used in the theoretical model.

Langley Research Center,
National Aeronautics and Space Administration,
Langley Station, Hampton, Va., October 1, 1964.

APPENDIX A

DESCRIPTIONS OF IBM 7094 COMPUTER PROGRAM FOR DETERMINING THIN-TARGET CROSS-SECTION DIFFERENTIAL WITH RESPECT TO PHOTON ENERGY AND ANGLE

GENERAL INFORMATION OF PROGRAM ONE

Purpose and Nomenclature

The purpose of this program is to compute the bremsstrahlung cross-section differential with respect to photon energy k and solid angle Ω_k. Required inputs for the program, along with the letter symbols used in the program, are as follows:

(1) Atomic number of target material (Z)
(2) Increment in angle θ_o (DDEG)
(3) Initial angle θ_o (THMIN)
(4) Final angle θ_o (THMAX)
(5) Initial photon energy (AKMIN)
(6) Increment in electron kinetic energy (DTMEV)
(7) Initial electron kinetic energy (TMIN)
(8) Final electron kinetic energy (TMAX)
(9) Constant for photon-energy increment (CONST)

The nomenclature used in program one is presented in table I.

Input Preparation and Output Description

Input data.- The input data for this program consist of three cards, as follows:

Card 1: Contains four program variables in a 4E12.4 format statement which are (1) the constant (CONST) that determines the increment in photon energy, (2) the initial photon energy (AKMIN), (3) the initial angle (THMIN), and (4) the final angle (THMAX).

Card 2: Contains four program variables in a 4E12.4 format statement which are (1) the final electron kinetic energy (TMAX), (2) the increment in angle θ_o (DDEG), (3) the increment in electron kinetic energy (DTMEV), and (4) the initial electron kinetic energy (TMIN).

Card 3: Contains the atomic number Z of the target element in an E12.4 format statement.

Output data.- The output data appear on a listing with appropriate headings and titles. The number following the E in each tabulated entry indicates the power of 10 by which that entry should be multiplied.

PROGRAM SEQUENCE

The program starts at an initial electron kinetic energy, and for an initial photon energy the cross section for all angles is calculated as specified.

The photon energy is then incremented from its initial value, and the cross sections for all angles are calculated again. This step is repeated until the photon energy reaches its upper limit, which is the electron kinetic energy.

Then the electron kinetic energy is incremented, the photon energy and the angle are reset to their initial values, and the cross sections for all angles are computed, and so forth.

The calculations are complete for a material of particular atomic number Z when the electron kinetic energy reaches its maximum, as specified in the input by TMAX.

The program calculations have been completed when there are no more materials to be read in.

The following program has been used on the IBM 7094 electronic data processing system at the Langley Research Center to obtain the results shown herein. Also included is a sample of the output data used.

```
C      PROGRAM NUMBER ONE(1)  REFERENCE EQUATION THREE(3)
C      TMIN MUST BE GREATER THAN AKMIN
C      AKMIN MUST BE GREATER THAN ZERO
C      TMAX MUST BE GREATER THAN TMIN
C      0 LESS THAN OR EQUAL TO THDEG LESS THAN OR EQUAL TO 180 DEGEEES
   50 FORMAT(1H1//////////95H THIN TARGET BREMSSTRAHLUNG CROSS-SECTIONS
     1DIFFERENTIAL WITH RESPECT TO PHOTON ENERGY AND ANGLE//)
   52 FORMAT(47X28H REFERENCE EQUATION THREE(3))
      WRITE OUTPUT TAPE 6,50
      WRITE OUTPUT TAPE 6,52
      READ INPUT TAPE 5,33,CONST,AKMIN,THMIN,THMAX
      READ INPUT TAPE 5,33,TMAX,DDEG,DTMEV,TMIN
    2 READ INPUT TAPE 5,54,Z
   33 FORMAT(4E12.4)
   54 FORMAT(E12.4)
      ROSQ=7.9524E-26
   88 FORMAT(1H1//////////44X32HATOMIC NUMBER OF TARGET MATERIAL//)
      WRITE OUTPUT TAPE 6,88
   99 FORMAT(58X,F6.2)
      WRITE OUTPUT TAPE 6,99,Z
      PIE=3.1415926
      DRAD=DDEG*0.017453
      DTO=DTMEV/.511
      TOMEV=TMIN
    6 AKMEV=AKMIN
   60 FORMAT(1H1//////////39X51HINCIDENT ELECTRON KINETIC ENERGY UPON TA
     1RGET IN MEV//)
      WRITE OUTPUT TAPE 6,60
      AK=AKMEV/.511
      DKMEV=TOMEV/CONST
      DK=DKMEV/.511
      TO=TOMEV/.511
   61 FORMAT(52X,F5.2)
      WRITE OUTPUT TAPE 6,61,TOMEV
    8 AK=AKMEV/.511
      THDEG=THMIN
   56 FORMAT(1H1,14X109HPHOTON      PHOTON        CROSS-SECTION WITH
     1 PHOTON ENERGY*CROSS-SECTION      PHOTON ENERGY*CROSS-SECTION)
   57 FORMAT(15X112HENERGY.     ANGLE     RESPECT TO PHOTON ENERGY
     1WITH RESPECT TO PHOTON     WITH RESPECT TO PHOTON ENERGY AND)
   58 FORMAT(40X85HAND SOLID ANGLE          ENERGY AND SOLID ANGLE
     1    SOLID ANGLE/ATOMIC NO.SQUARED//)
   62 FORMAT(16X100HMEV       DEGREES       SQ.CM/MEV-STERAD
     1 SQ.CM/STERAD                        SQ.CM/STERAD //)
      WRITE OUTPUT TAPE 6,56
      WRITE OUTPUT TAPE 6,57
      WRITE OUTPUT TAPE 6,58
      WRITE OUTPUT TAPE 6,62
   10 THRAD=THDEG*0.017453
```

```
      EO=TO+1.
      EOSQ=EO**2.
      E=EO-AK
      ESQ=E**2.
      PO=SQRTF(TO*(TO+2.))
      POSQ=PO**2.
      T=E-1.
      P=SQRTF(T*(T+2.))
      PSQ=P**2.
      AL=LOGF(((E*EO)-1.+(P*PO))/((E*EO)-1.-(P*PO)))
      DELTA=EO-(PO*COSF(THRAD))
      DELSQ=(EO-(PO*COSF(THRAD)))**2.
      EPSN=LOGF((E+P)/(E-P))
      AKSQ=AK**2.
      QSQ=POSQ+AKSQ-(2.*PO*AK*COSF(THRAD))
      Q=SQRTF(QSQ)
      EPSNQ=LOGF((Q+P)/(Q-P))
      R1=(4./DELSQ)-((6.*AK)/DELTA)-((2.*AK)*(POSQ-AKSQ))/(QSQ*DELTA)
      R2=(EPSNQ/(P*Q))*R1
      R3=(4.*EPSN)/(P*DELTA)
      S9=4.*EO*((SINF(THRAD))**2)
      R4=S9*(((3.*AK)-(POSQ*E))/(POSQ*(DELSQ**2.)))
      R5=((4.*EOSQ)*(EOSQ+ESQ))/(POSQ*DELSQ)
      R6=(2.-(2.*((7.*EOSQ)-(3.*E*EO)+ESQ)))/(POSQ*DELSQ)
      R7=(2.*AK*(EOSQ+(E*EO)-1.))/(POSQ*DELTA)
      R8=(AL*(R4+R5+R6+R7))/(P*PO)
      R9=R8-R3+R2
      S1=(8.*((SINF(THRAD))**2.))*((2.*EOSQ)+1.)/(POSQ*(DELSQ**2.))
      S2=(2.*((5.*EOSQ)+(2.*E*EO)+3.)/(POSQ*DELSQ))
      S3=(2.*(POSQ-AKSQ))/(QSQ*DELSQ)
      S4=(4.*E)/(POSQ*DELTA)
      S5=S1-S2-S3+S4+R9
      S6=(ROSQ*P*S5)/(8.*PIE*137.*PO)
      S7=((Z**2.)*S6)/AK
      S8=S7/0.511
      T4=(S8*AKMEV)/(Z**2.)
      B11=AKMEV*S8
   80 FORMAT(1X,F20.4,F12.1,E22.8,E28.8,E36.8)
      WRITE OUTPUT TAPE 6,80,AKMEV,THDEG,S8,B11,T4
      THDEG=THDEG+DDEG
      IF(THMAX-THDEG)91,10,10
   91 AKMEV=AKMEV+DKMEV
      IF(TOMEV-AKMEV)92,92,44
   44 IF(ABSF(TOMEV-AKMEV)-.0001)92,92,8
   92 TOMEV=TOMEV+DTMEV
      IF(TMAX-TOMEV)40,6,6
   40 GO TO 2
      END
```

OUTPUT DATA FOR PROGRAM ONE

THIN-TARGET BREMSSTRAHLUNG CROSS-SECTIONS DIFFERENTIAL WITH RESPECT TO PHOTON ENERGY AND ANGLE

REFERENCE EQUATION THREE

ATOMIC NUMBER OF TARGET MATERIAL

6.00

INCIDENT ELECTRON KINETIC ENERGY UPON TARGET IN MEV

1.00

PHOTON ENERGY	PHOTON ANGLE	CROSS SECTION WITH RESPECT TO PHOTON ENERGY AND SOLID ANGLE	PHOTON ENERGY*CROSS SECTION WITH RESPECT TO PHOTON ENERGY AND SOLID ANGLE	PHOTON ENERGY*CROSS SECTION WITH RESPECT TO PHOTON ENERGY AND SOLID ANGLE/ATOMIC NO.SQUARED
MEV	DEGREES	SQ.CM/MEV-STERAD	SQ.CM/STERAD	SQ.CM/STERAD
0.1000	0.	0.15065948E-22	0.15065947E-23	0.41849855E-25
0.1000	30.0	0.10669796E-23	0.10669796E-24	0.29638324E-26
0.1000	60.0	0.14878167E-24	0.14878167E-25	0.41328245E-27
0.1000	90.0	0.40620318E-25	0.40620318E-26	0.11283422E-27
0.1000	120.0	0.17513111E-25	0.17513111E-26	0.48647532E-28
0.1000	150.0	0.10795724E-25	0.10795724E-26	0.29988122E-28
0.1000	180.0	0.92065404E-26	0.92065403E-27	0.25573724E-28
0.2000	0.	0.53353585E-23	0.10670716E-23	0.29640881E-25
0.2000	30.0	0.40074071E-24	0.80148140E-25	0.22263373E-26
0.2000	60.0	0.51632897E-25	0.10326579E-25	0.28684942E-27
0.2000	90.0	0.13560308E-25	0.27120616E-26	0.75335047E-28
0.2000	120.0	0.56902461E-26	0.11380492E-26	0.31612479E-28
0.2000	150.0	0.34414387E-26	0.68828773E-27	0.19119104E-28
0.2000	180.0	0.29136743E-26	0.58273487E-27	0.16187080E-28
0.3000	0.	0.26496799E-23	0.79490398E-24	0.22080667E-25
0.3000	30.0	0.21101160E-24	0.63303478E-25	0.17584299E-26
0.3000	60.0	0.25162940E-25	0.75488819E-26	0.20969117E-27
0.3000	90.0	0.63894464E-26	0.19168339E-26	0.53245386E-28
0.3000	120.0	0.26235433E-26	0.78706298E-27	0.21862861E-28
0.3000	150.0	0.15619544E-26	0.46858631E-27	0.13016286E-28
0.3000	180.0	0.13142825E-26	0.39428475E-27	0.10952354E-28
0.4000	0.	0.14944444E-23	0.59777774E-24	0.16604938E-25
0.4000	30.0	0.12692229E-24	0.50768915E-25	0.14102476E-26
0.4000	60.0	0.13984845E-25	0.55939380E-26	0.15538717E-27
0.4000	90.0	0.34373675E-26	0.13749470E-26	0.38192973E-28
0.4000	120.0	0.13805567E-26	0.55222267E-27	0.15339519E-28
0.4000	150.0	0.80771907E-27	0.32308762E-27	0.89746564E-29
0.4000	180.0	0.67479853E-27	0.26991941E-27	0.74977616E-29
0.5000	0.	0.88966388E-24	0.44483193E-24	0.12356442E-25
0.5000	30.0	0.81534375E-25	0.40767187E-25	0.11324219E-26
0.5000	60.0	0.82971770E-26	0.41485884E-26	0.11523856E-27
0.5000	90.0	0.19696943E-26	0.98484718E-27	0.27356866E-28
0.5000	120.0	0.76951935E-27	0.38475966E-27	0.10687768E-28
0.5000	150.0	0.43961209E-27	0.21980604E-27	0.61057235E-29
0.5000	180.0	0.36355779E-27	0.18177889E-27	0.50494137E-29
0.6000	0.	0.53523845E-24	0.32114306E-24	0.89206409E-26
0.6000	30.0	0.54111499E-25	0.32466899E-25	0.90185831E-27
0.6000	60.0	0.50996410E-26	0.30597845E-26	0.84994017E-28
0.6000	90.0	0.11611781E-26	0.69670688E-27	0.19352970E-28
0.6000	120.0	0.43602613E-27	0.26161567E-27	0.72671022E-29
0.6000	150.0	0.24008945E-27	0.14405367E-27	0.40014909E-29
0.6000	180.0	0.19533712E-27	0.11720227E-27	0.32556187E-29
0.7000	0.	0.31124862E-24	0.21787402E-24	0.60520563E-26
0.7000	30.0	0.36258280E-25	0.25380795E-25	0.70502211E-27
0.7000	60.0	0.31843037E-26	0.22290125E-26	0.61917017E-28
0.7000	90.0	0.68636778E-27	0.48045743E-27	0.13346040E-28
0.7000	120.0	0.24260125E-27	0.16982087E-27	0.47172465E-29
0.7000	150.0	0.12561578E-27	0.87931044E-28	0.24425291E-29
0.7000	180.0	0.99265864E-28	0.69486102E-28	0.19301695E-29
0.8000	0.	0.16157174E-24	0.12925739E-24	0.35904831E-26
0.8000	30.0	0.23860612E-25	0.19088488E-25	0.53023580E-27
0.8000	60.0	0.19673527E-26	0.15738821E-26	0.43718949E-28
0.8000	90.0	0.39355490E-27	0.31484392E-27	0.87456645E-29
0.8000	120.0	0.12652574E-27	0.10122059E-27	0.28116831E-29
0.8000	150.0	0.58575446E-28	0.46860355E-28	0.13016766E-29
0.8000	180.0	0.43583415E-28	0.34866731E-28	0.96852033E-30
0.9000	0.	0.58525499E-25	0.52672947E-25	0.14631374E-26
0.9000	30.0	0.14259923E-25	0.12833930E-25	0.35649806E-27
0.9000	60.0	0.11081039E-26	0.99729350E-27	0.27702598E-28
0.9000	90.0	0.20074087E-27	0.18066677E-27	0.50185218E-29
0.9000	120.0	0.55494872E-28	0.49945383E-28	0.13873717E-29
0.9000	150.0	0.20269742E-28	0.18242767E-28	0.50674354E-30
0.9000	180.0	0.12724185E-28	0.11451766E-28	0.31810462E-30

APPENDIX B

DESCRIPTIONS OF IBM 7094 COMPUTER PROGRAM FOR DETERMINING THIN-TARGET CROSS-SECTION DIFFERENTIAL WITH RESPECT TO PHOTON ENERGY

GENERAL INFORMATION ON PROGRAM TWO

Purpose and Nomenclature

The purpose of this program is to compute the bremsstrahlung cross-section differential with respect to the photon energy k. Required inputs for the program, along with the letter symbols used in the program, are as follows:

(1) Atomic number of target material (Z)
(2) Increment in electron kinetic energy (DTMEV)
(3) Initial electron kinetic energy (TMIN)
(4) Final electron kinetic energy (TMAX)
(5) Initial photon energy (AKMIN)
(6) Constant for photon-energy increment (CONST)

The nomenclature used in program two is presented in table II.

Input Preparation and Output Description

Input data.- The input data for this program consist of two cards, as follows:

Card 1: Contains five program variables which are (1) the constant (CONST) for the photon-energy increment, (2) the increment in electron kinetic energy (DTMEV), (3) the initial electron kinetic energy (TMIN), (4) the final electron kinetic energy (TMAX), and (5) the initial photon energy (AKMIN), in a 5E12.4 format.

Card 2: Contains the atomic number Z of the target element, in an E12.4 format.

Output data.- The output data appear on a listing with appropriate headings and titles. The number following the E in each tabulated entry indicates the power of 10 by which that entry should be multiplied.

PROGRAM SEQUENCE

The program starts at an initial electron kinetic energy and an initial photon energy. The photon energy is incremented from its initial value, and

the cross section for each photon energy is calculated to its upper limit, which is the electron kinetic energy.

The electron kinetic energy is then incremented, and the photon energy is reset to the initial value. Again, the photon energy is incremented from the initial value, with the cross section for each photon energy being calculated.

The calculations are complete for a material of particular atomic number Z when the electron kinetic energy reaches its maximum, as specified in the input by TMAX.

The program calculations have been completed when there are no more materials to be read in.

The following program has been used on the IBM 7094 electronic data processing system at the Langley Research Center to obtain the results shown herein. Also included is a sample of the output data used.

```
C       PROGRAM NUMBER TWO(2)  REFERENCE EQUATION FOUR(4)
C       THIN TARGET BREMSSTRAHLUNG CROSS SECTIONS
C       TMAX MUST BE GREATER THAN TMIN
C       TMIN MUST BE GREATER THAN AKMIN
C       AKMIN MUST BE GREATER THAN ZERO
   50 FORMAT(1H1//////////25X72HBREMSSTRAHLUNG CROSS-SECTIONS DIFFERENTI
     1AL WITH RESPECT TO PHOTON ENERGY//)
   52 FORMAT(58X26HREFERENCE EQUATION FOUR(4))
      WRITE OUTPUT TAPE 6,50
      WRITE OUTPUT TAPE 6,52
      READ INPUT TAPE 5,33,CONST,DTMEV,TMIN,TMAX,AKMIN
   80 READ INPUT TAPE 5,54,Z
   33 FORMAT(5E12.4)
   54 FORMAT(E12.4)
   58 FORMAT(1H1//////////44X32HATOMIC NUMBER OF TARGET MATERIAL//)
      WRITE OUTPUT TAPE 6,58
   99 FORMAT(58X,F6.2)
      WRITE OUTPUT TAPE 6,99,Z
      ROSQ=7.9524E-26
      TOMEV = TMIN
   30 TO=TOMEV/.511
   60 FORMAT(1H1/45X52H INCIDENT ELECTRON KINETIC ENERGY UPON TARGET IN
     1MEV//)
   61 FORMAT(59X,F11.4)
      WRITE OUTPUT TAPE 6,60
      WRITE OUTPUT TAPE 6,61,TOMEV
      AKMEV=AKMIN
      DKMEV=TOMEV/CONST
   70 FORMAT(/20X96HPHOTON ENERGY       CROSS-SECTION       PHOTON ENERGY*
     1C-SEC       PHOTON ENERGY*CROSS-SECTION/Z.SQ.//)
   71 FORMAT(25X78HMEV              MILLI-B/MEV             MILLIBARNS
     1                MILLIBARNS//)
      WRITE OUTPUT TAPE 6,70
      WRITE OUTPUT TAPE 6,71
   10 AK=AKMEV/.511
      EO=TO+1.0
   72 FORMAT(1X,F29.4,E22.8,E22.8,E31.8)
      CROSS=CROSEC(EO,AK)/1.00E-27
      T1=CROSS*(Z**2.)
      T2=T1/AKMEV
      WRITE OUTPUT TAPE 6,72,AKMEV,T2,T1,CROSS
      AKMEV=AKMEV+DKMEV
      IF(TOMEV-AKMEV)20,20,44
   44 IF(ABSF(TOMEV-AKMEV)-.0001)20,20,10
   20 TOMEV=TOMEV+DTMEV
      IF(TMAX-TOMEV)80,30,30
      END
      FUNCTION CROSEC(EO,AK)
C     FUNCTION CROSEC(EO,AK) IS A SUBPROGRAM OF PROGRAM TWO(2)
```

```
C  FUNCTION CROSEC(EO,AK) EVALUATES EQUATION FOUR(4)
C  EO AND AK MUST BE IN MC**2 UNITS
   ROSQ = 7.9524E-26
   E=EO-AK
   TO = EO-1.
   T = E-1.
   IF(T) 1,1,2
 1 CROSEC = 0.
 3 RETURN
 2 POSQ = TO*(TO+2.)
   POSQ = TO*(TO+2.)
   PO = SQRTF(POSQ)
   POQD = PO*POSQ
   PSQ = T*(T+2.)
   P = SQRTF(PSQ)
   PQD = P*PSQ
   PP = P*PO
   PPSQ = POSQ*PSQ
   PPQD = POQD*PQD
   EOE = EO*E
   FO = LOGF((EO+PO)/(EO-PO))
   F = LOGF((E+P)/(E-P))
   AL = 2.*LOGF((EOE+PP-1.)/AK)
C
   CURLY = (EOE+POSQ)/POQD*FO-(EOE+PSQ)/PQD*F+2.*AK*EOE/PPSQ
   BRAKT = 8./3.*EOE/PP+AK**2/PPQD*(EOE**2+PPSQ)+AK/2.*CURLY/PP
   BRACE = 4./3.-2.*EOE/PPSQ*(PSQ+POSQ)+FO/POQD*E+F/PQD*EO-F*FO/PP
  1          +AL*BRAKT
   CROSEC = ROSQ/137.*P/PO*BRACE
   GO TO 3
   END
```

OUTPUT DATA FOR PROGRAM TWO

THIN-TARGET BREMSSTRAHLUNG CROSS-SECTIONS DIFFERENTIAL WITH RESPECT TO PHOTON ENERGY

REFERENCE EQUATION FOUR

ATOMIC NUMBER OF TARGET MATERIAL

6.00

INCIDENT ELECTRON KINETIC ENERGY UPON TARGET IN MEV

1.00

PHOTON ENERGY MEV	CROSS SECTION MILLIBARNS/MEV	PHOTON ENERGY*CROSS SECTION MILLIBARNS	PHOTON ENERGY*CROSS SECTION/Z.SQ. MILLIBARNS
0.1000	0.43164050E 04	0.43164051E 03	0.11990014E 02
0.2000	0.15958299E 04	0.31916598E 03	0.88657220E 01
0.3000	0.82923023E 03	0.24876907E 03	0.69102520E 01
0.4000	0.49269348E 03	0.19707739E 03	0.54743721E 01
0.5000	0.31251367E 03	0.15625683E 03	0.43404678E 01
0.6000	0.20413920E 03	0.12248352E 03	0.34023201E 01
0.7000	0.13343827E 03	0.93406790E 02	0.25946331E 01
0.8000	0.83999594E 02	0.67199674E 02	0.18666577E 01
0.9000	0.46292787E 02	0.41663507E 02	0.11573196E 01

INCIDENT ELECTRON KINETIC ENERGY UPON TARGET IN MEV

1.10

PHOTON ENERGY MEV	CROSS SECTION MILLIBARNS/MEV	PHOTON ENERGY*CROSS SECTION MILLIBARNS	PHOTON ENERGY*CROSS SECTION/Z.SQ. MILLIBARNS
0.1000	0.44435771E 04	0.44435771E 03	0.12343270E 02
0.2100	0.15518689E 04	0.32589248E 03	0.90525690E 01
0.3200	0.79220642E 03	0.25350605E 03	0.70418350E 01
0.4300	0.46706106E 03	0.20083625E 03	0.55787849E 01
0.5400	0.29530442E 03	0.15946438E 03	0.44295664E 01
0.6500	0.19286101E 03	0.12535965E 03	0.34822128E 01
0.7600	0.12641110E 03	0.96072436E 02	0.26686788E 01
0.8700	0.80153263E 02	0.69733338E 02	0.19370372E 01
0.9800	0.45128056E 02	0.44225495E 02	0.12284859E 01
1.0900	0.10129671E 02	0.11041341E 02	0.30670394E-00

REFERENCES

1. Hess, W. N.: The Artificial Radiation Belt Made on July 9, 1962. J. Geophys. Res., vol. 68, no. 3, Feb. 1, 1963, pp. 667-683.

2. Koch, H. W.; and Motz, J. W.: Bremsstrahlung Cross-Section Formulas and Related Data. Rev. Mod. Phys., vol. 31, no. 4, Oct. 1959, pp. 920-955.

3. Heitler, W.: The Quantum Theory of Radiation. Third ed., The Clarendon Press (Oxford), 1954, pp. 242-256.

4. Starfelt, N.; and Koch, H. W.: Differential Cross-Section Measurements of Thin-Target Bremsstrahlung Produced by 2.7- to 9.7-Mev Electrons. Phys. Rev., vol. 102, no. 6, June 15, 1956, pp. 1598-1612.

5. Evans, Robley D.: The Atomic Nucleus. McGraw-Hill Book Co., Inc., c.1955.

6. Bethe, Hans A.; and Ashkin, Julius: Passage of Radiations Through Matter. Experimental Nuclear Physics, Vol. I, E. Segrè, ed., John Wiley & Sons, Inc., c.1953, pp. 166-357.

TABLE I.- NOMENCLATURE USED IN APPENDIX A

Mathematical symbol	Program symbol	Definition	Units
Z	Z	Atomic charge number of target material	
r_o^2	ROSQ	Classical electron radius, squared	cm^2
$d\theta_o$	DDEG DRAD	Increment in angle θ_o	deg radians
	THMIN	Initial angle θ_o	deg
	THMAX	Final angle θ	deg
θ_o	THDEG THRAD	Photon emission angle	deg radians
T_o	TOMEV TO	Initial electron kinetic energy	MeV m_oc^2
	TMAX	Final electron kinetic energy	MeV
dT_o	DTMEV	Electron-kinetic-energy increment	MeV
	TMIN	Initial electron kinetic energy	MeV
	AKMIN	Initial photon energy	MeV
k	AKMEV	Photon energy	MeV
dk	DKMEV DK	Photon-energy increment (TOMEV/CONST) Photon-energy increment	MeV m_oc^2
	CONST	Constant used in determining photon-energy increment	
E_o	EO	Initial total electron energy (TO + 1)	m_oc^2
π	PIE	3.14159265	
$\frac{d\sigma}{dk\ d\Omega_k}$	S8	Differential bremsstrahlung cross section	cm^2/MeV-sr
$\frac{k}{dk}\frac{d\sigma}{d\Omega_k}$	B11	Photon energy times differential bremsstrahlung cross section	cm^2/sr
$\frac{k}{Z^2}\frac{d\sigma}{dk\ d\Omega_k}$	T4	Photon energy times differential bremsstrahlung cross section divided by atomic charge number, squared	cm^2/sr

TABLE II.- NOMENCLATURE USED IN APPENDIX B

Mathematical symbol	Program symbol	Definition	Units
Z	Z	Atomic charge number of target material	
r_o^2	ROSQ	Classical electron radius, squared	cm^2
dT_o	DTMEV	Electron-kinetic-energy increment	MeV
T_o	TMIN	Initial electron kinetic energy	MeV
	TOMEV		MeV
	TO		m_oc^2
	TMAX	Final electron kinetic energy	MeV
	AKMIN	Initial photon energy	MeV
k	AKMEV	Photon energy	MeV
	AK		m_oc^2
dk	DKMEV	Photon-energy increment	MeV
E_o	EO	Initial total electron energy (TO + 1)	m_oc^2
$\frac{d\sigma}{dk}$	T2	Differential bremsstrahlung cross section	m/MeV
$\frac{k\,d\sigma}{dk}$	T1	Photon energy times differential bremsstrahlung cross section	mb
$\frac{k}{Z^2}\frac{d\sigma}{dk}$	CROSS	Photon energy times differential bremsstrahlung cross section divided by atomic charge number, squared	mb

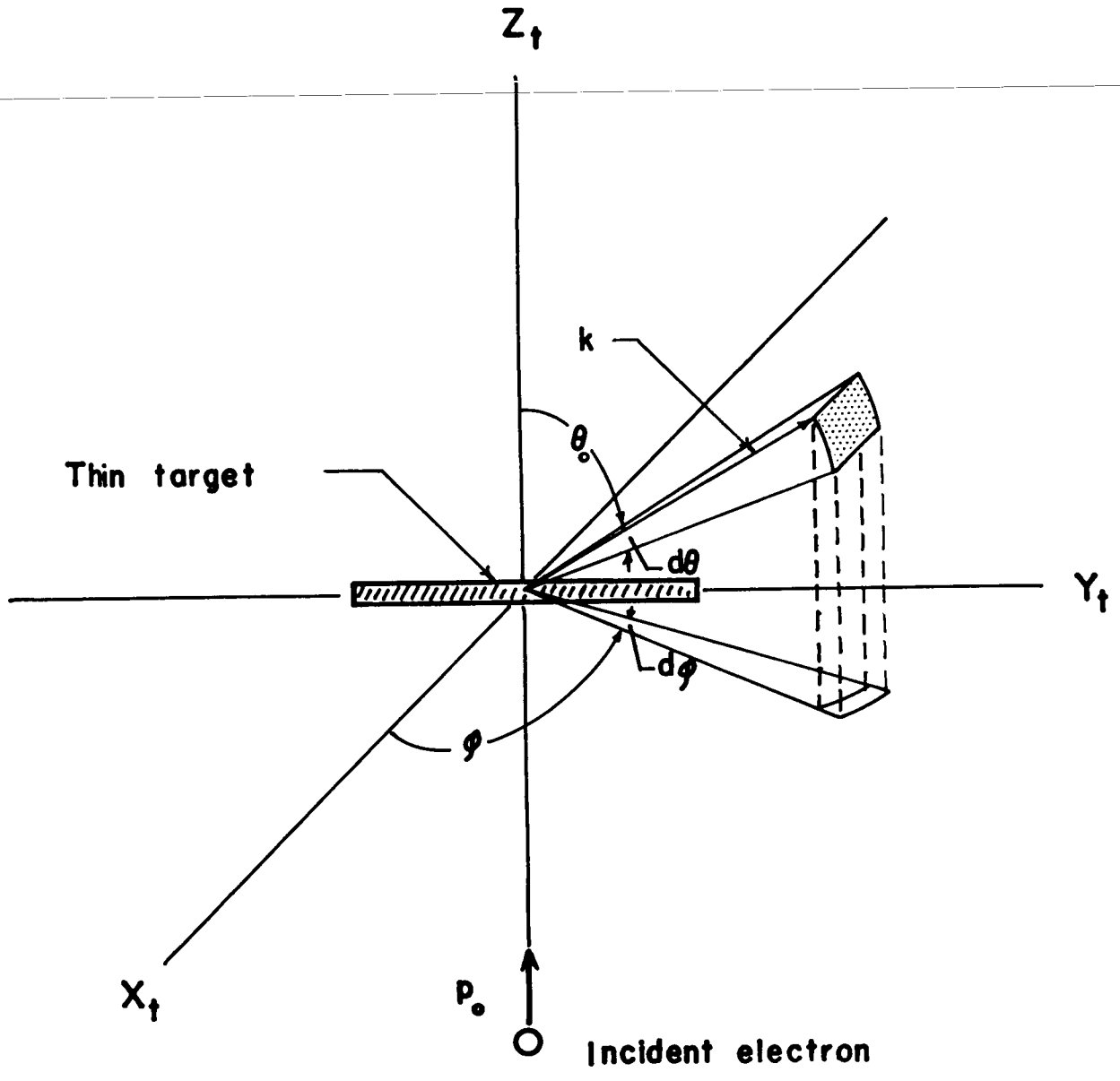

Figure 1.- Collision geometry.

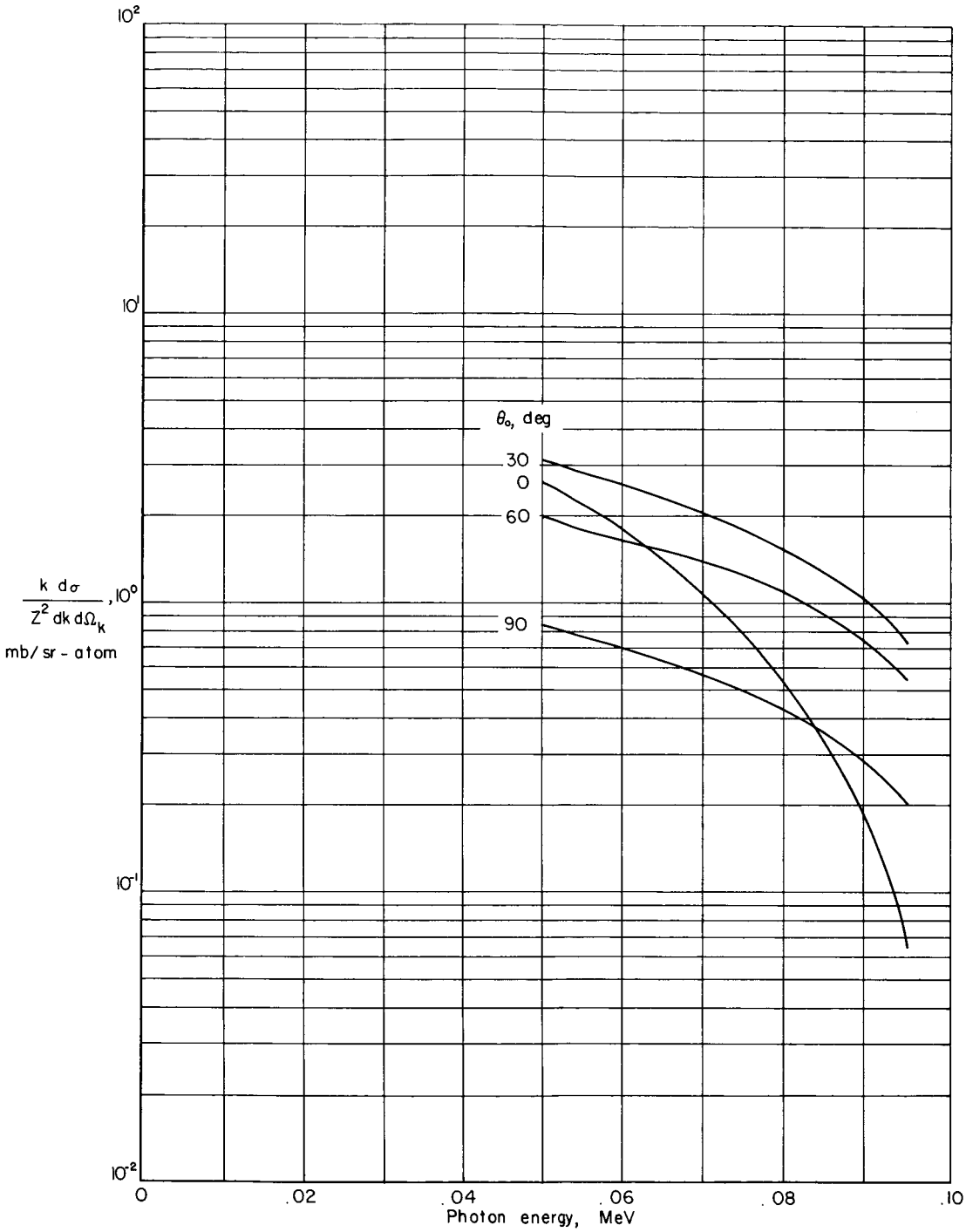

(a) Electron kinetic energy, 0.1 MeV.

Figure 2.- Dependence of thin-target bremsstrahlung intensity spectra on photon energy k, angle θ_o, and incident-electron kinetic energy.

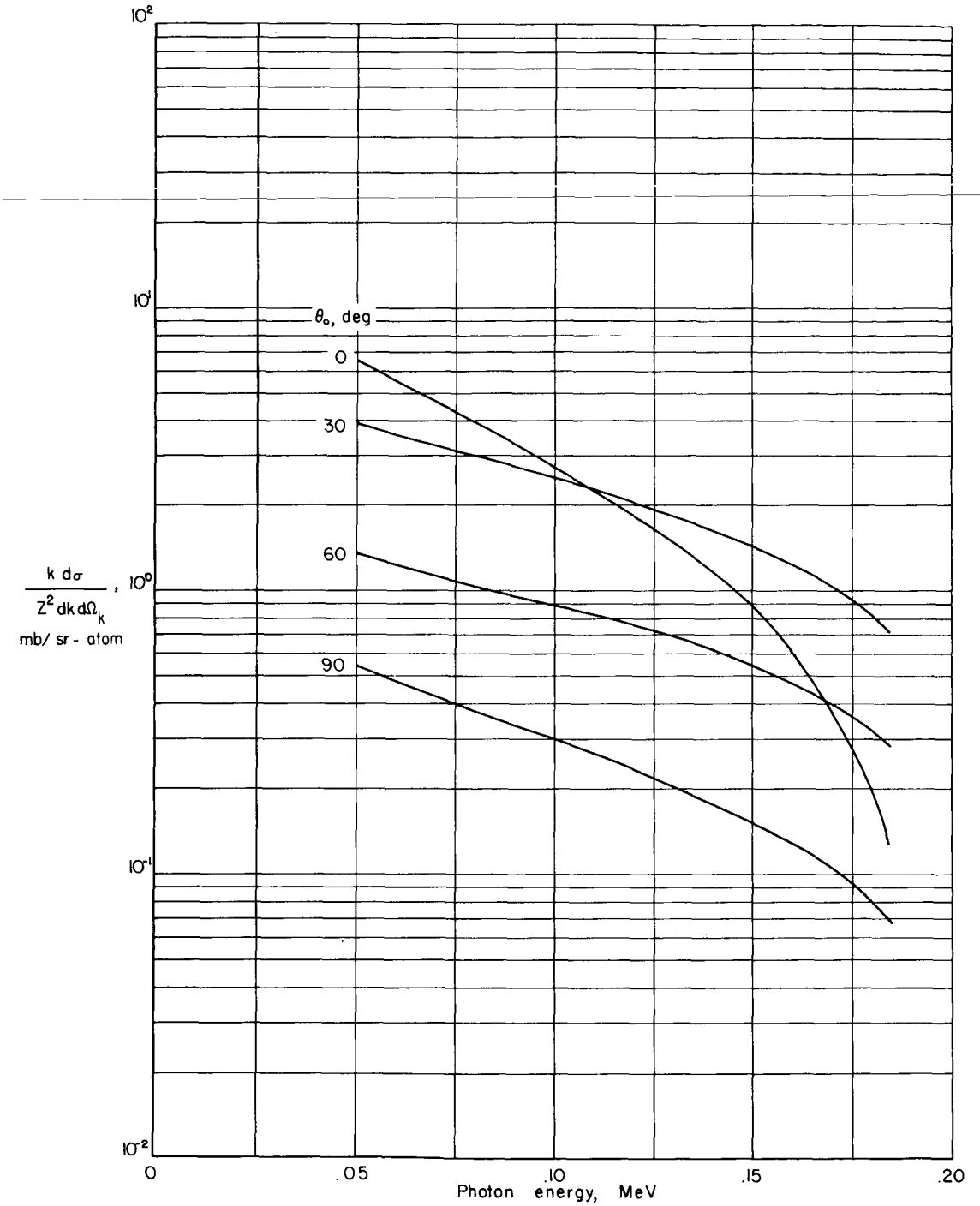

(b) Electron kinetic energy, 0.2 MeV.

Figure 2.- Continued.

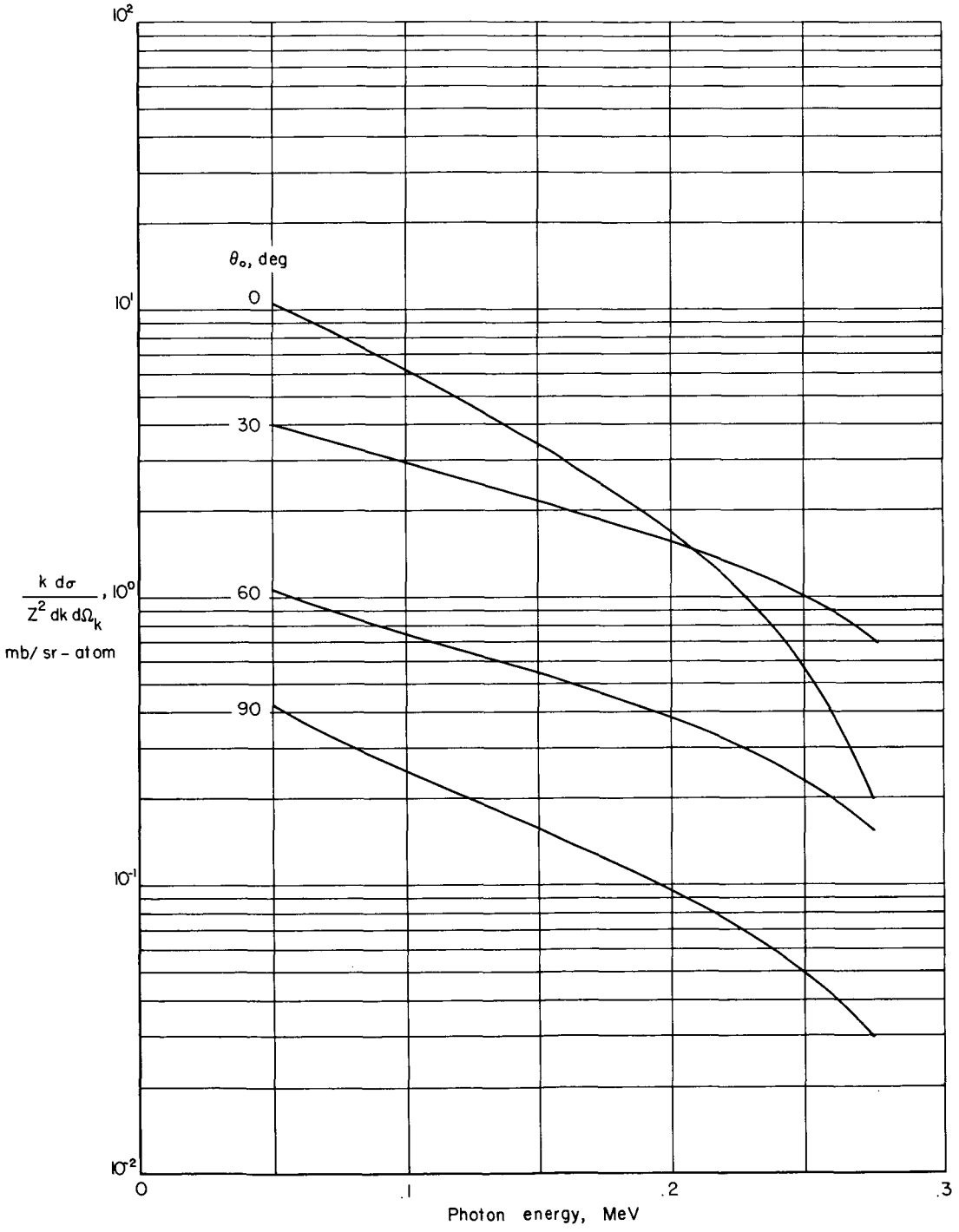

(c) Electron kinetic energy, 0.3 MeV.

Figure 2.- Continued.

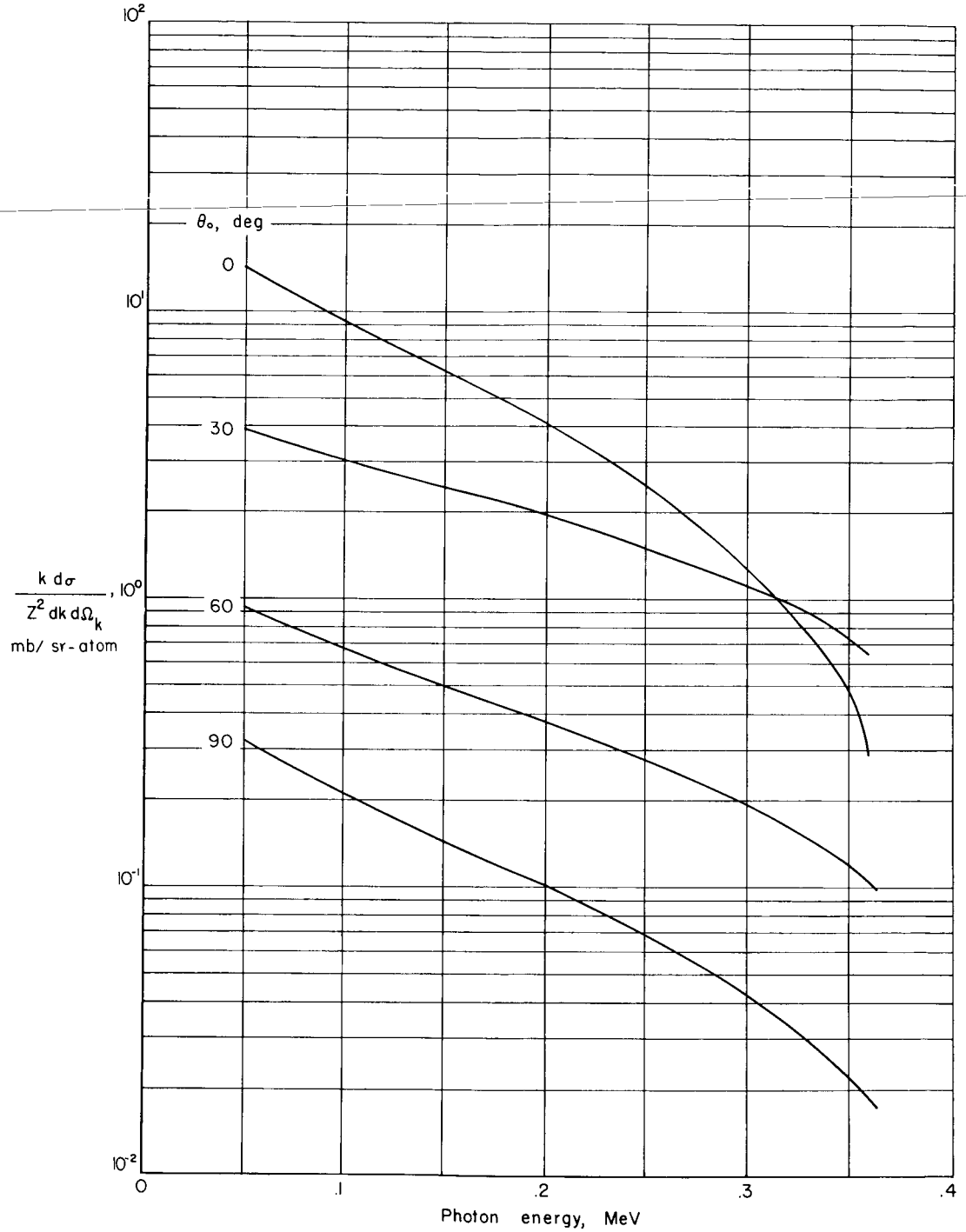

(d) Electron kinetic energy, 0.4 MeV.

Figure 2.- Continued.

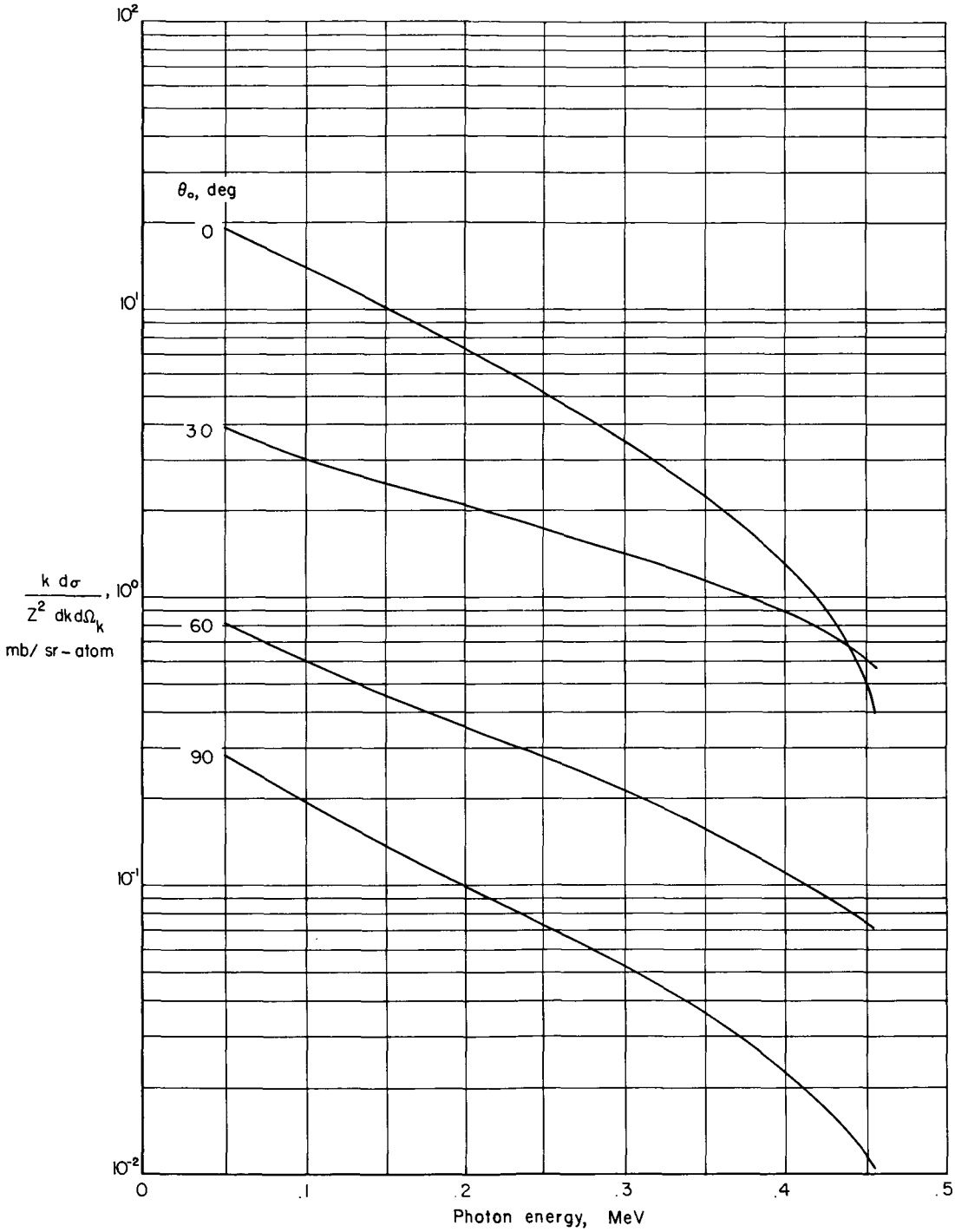

(e) Electron kinetic energy, 0.5 MeV.

Figure 2.- Continued.

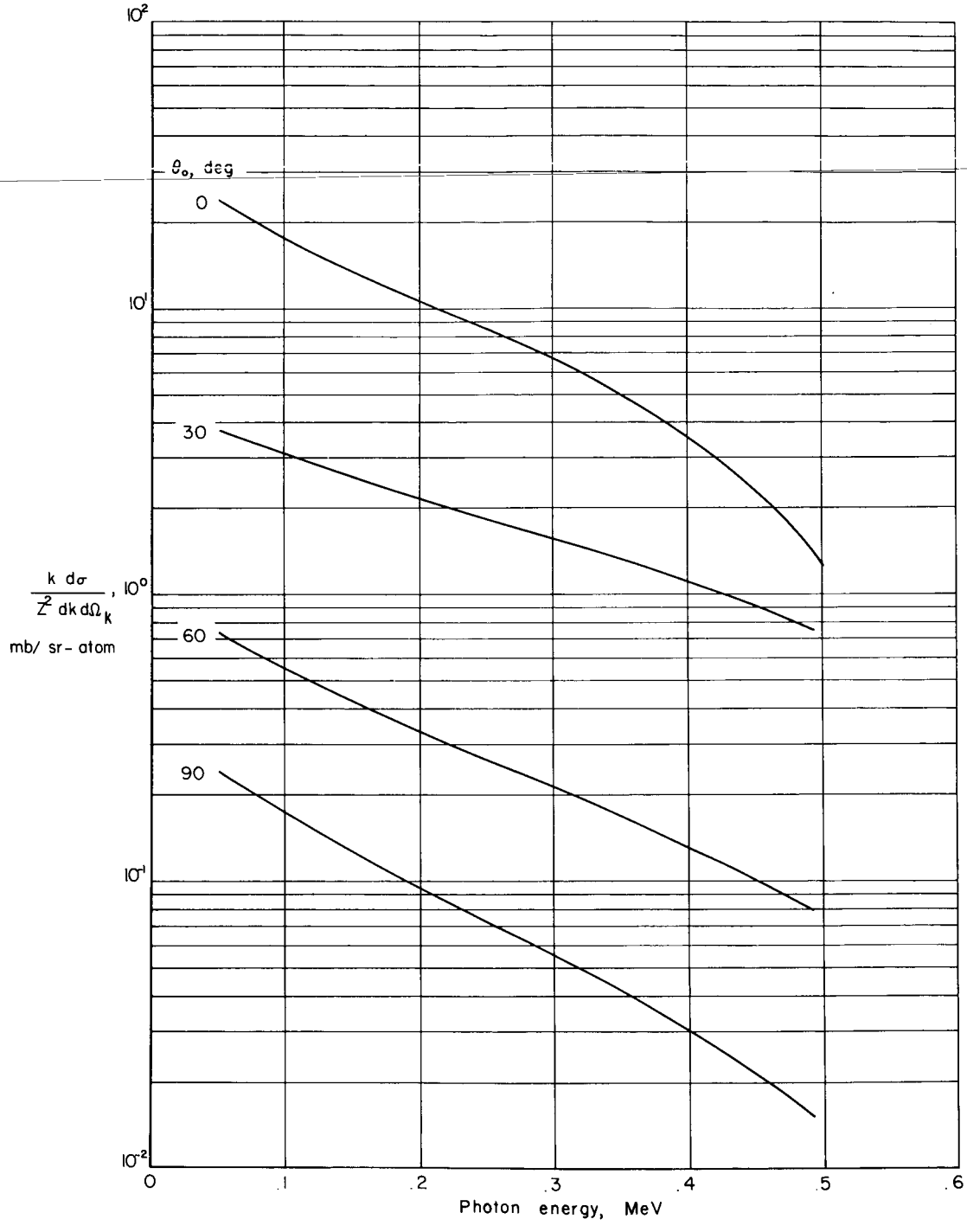

(f) Electron kinetic energy, 0.6 MeV.

Figure 2.- Continued.

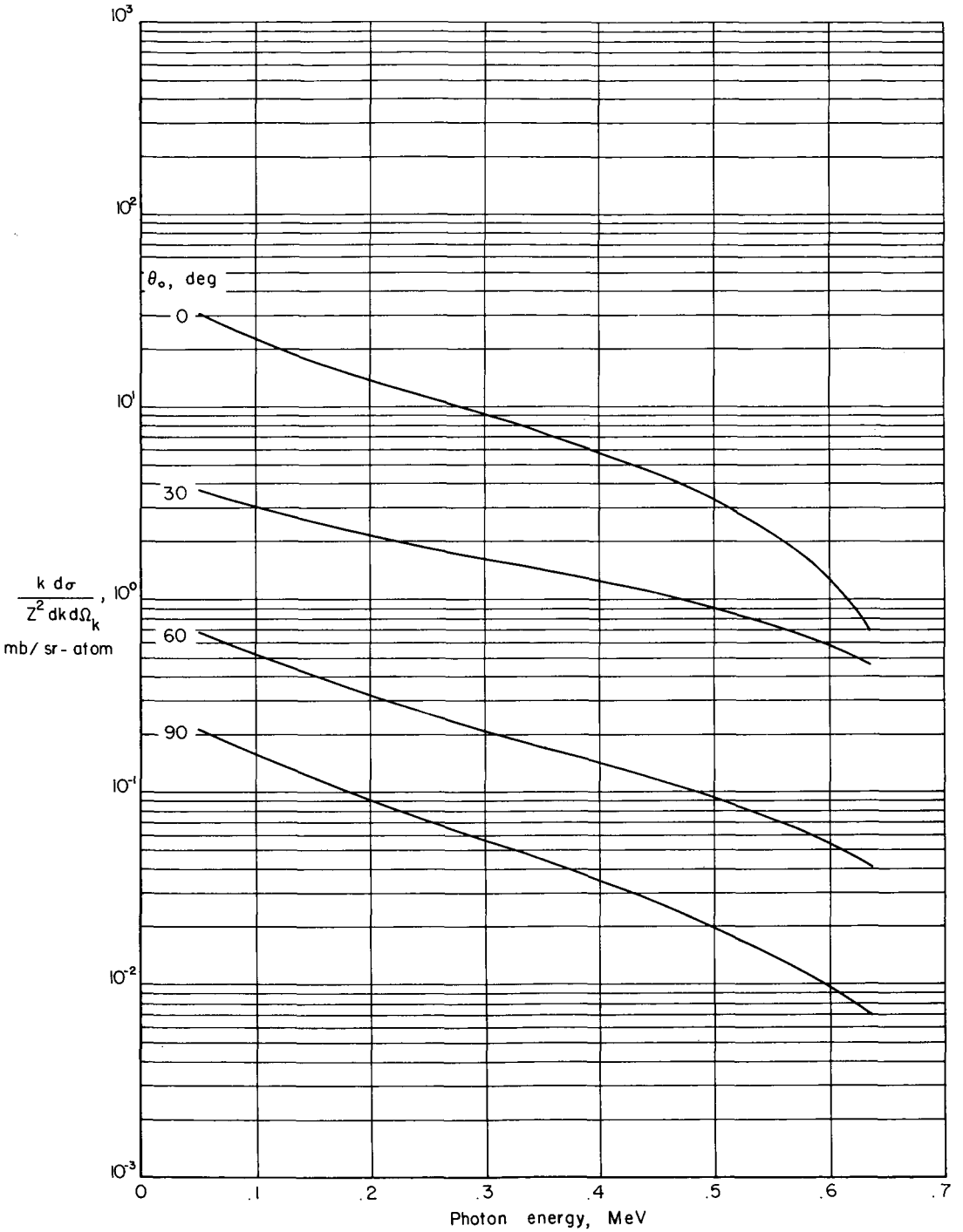

(g) Electron kinetic energy, 0.7 MeV.

Figure 2.- Continued.

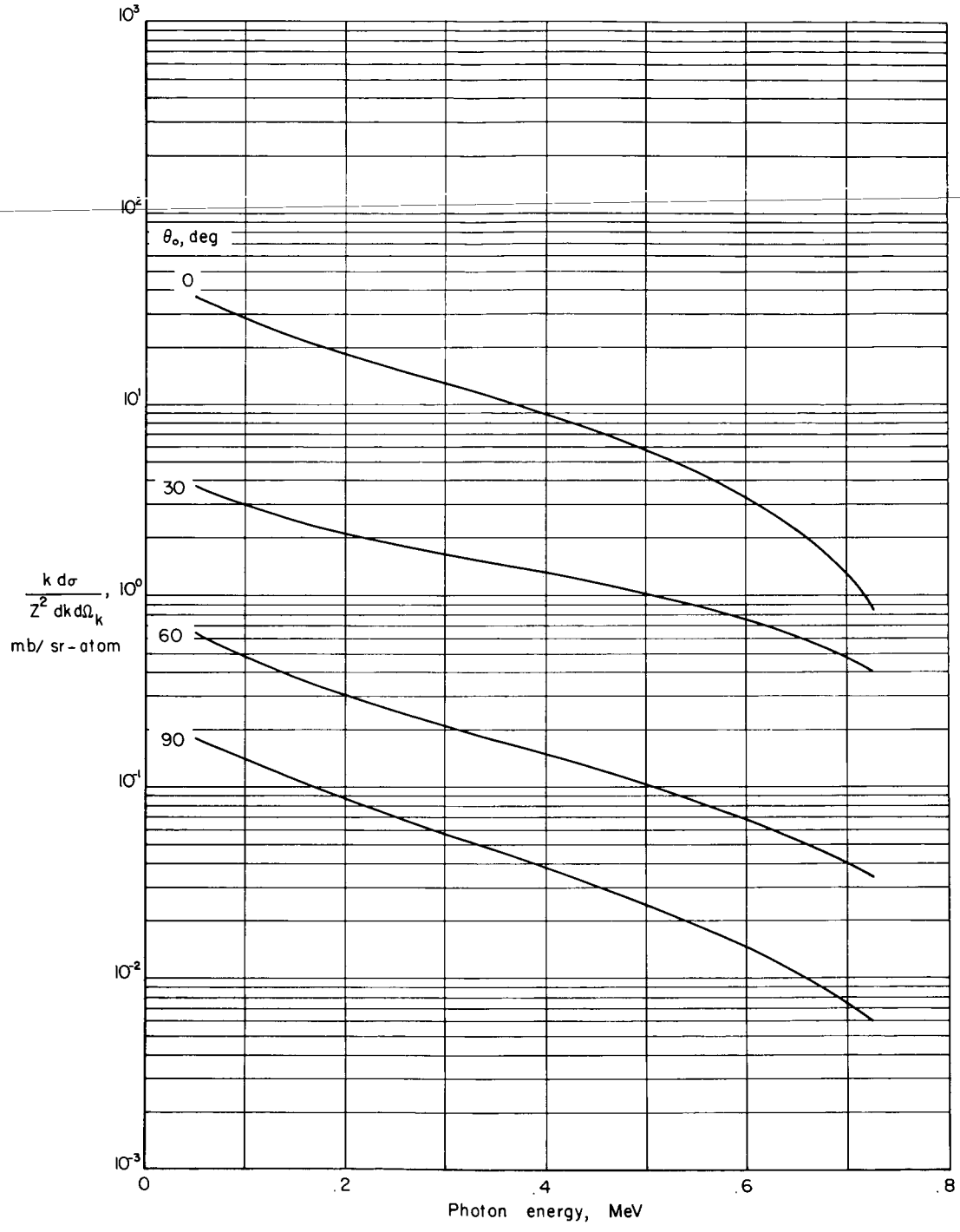

(h) Electron kinetic energy, 0.8 MeV.

Figure 2.- Continued.

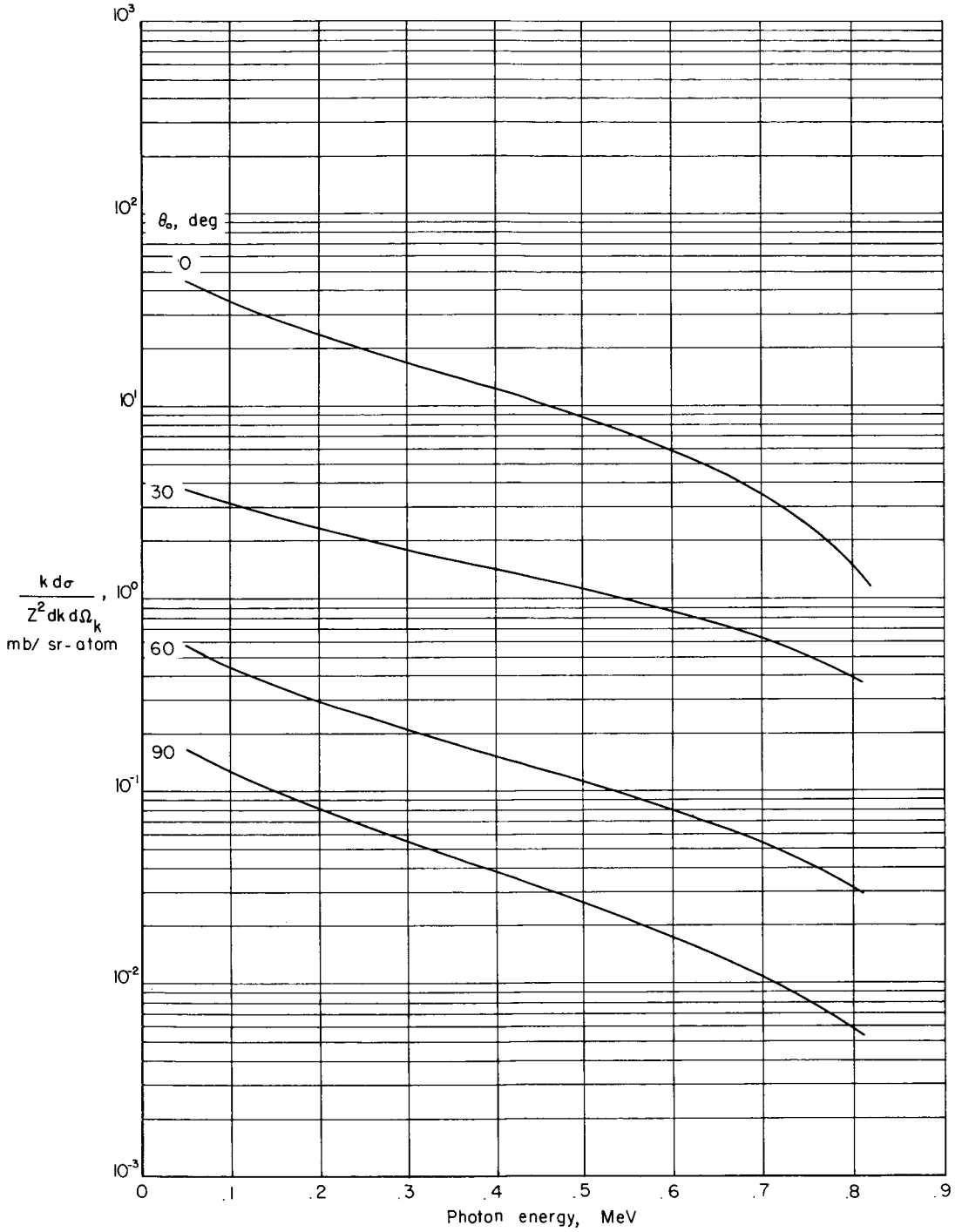

(i) Electron kinetic energy, 0.9 MeV.

Figure 2.- Continued.

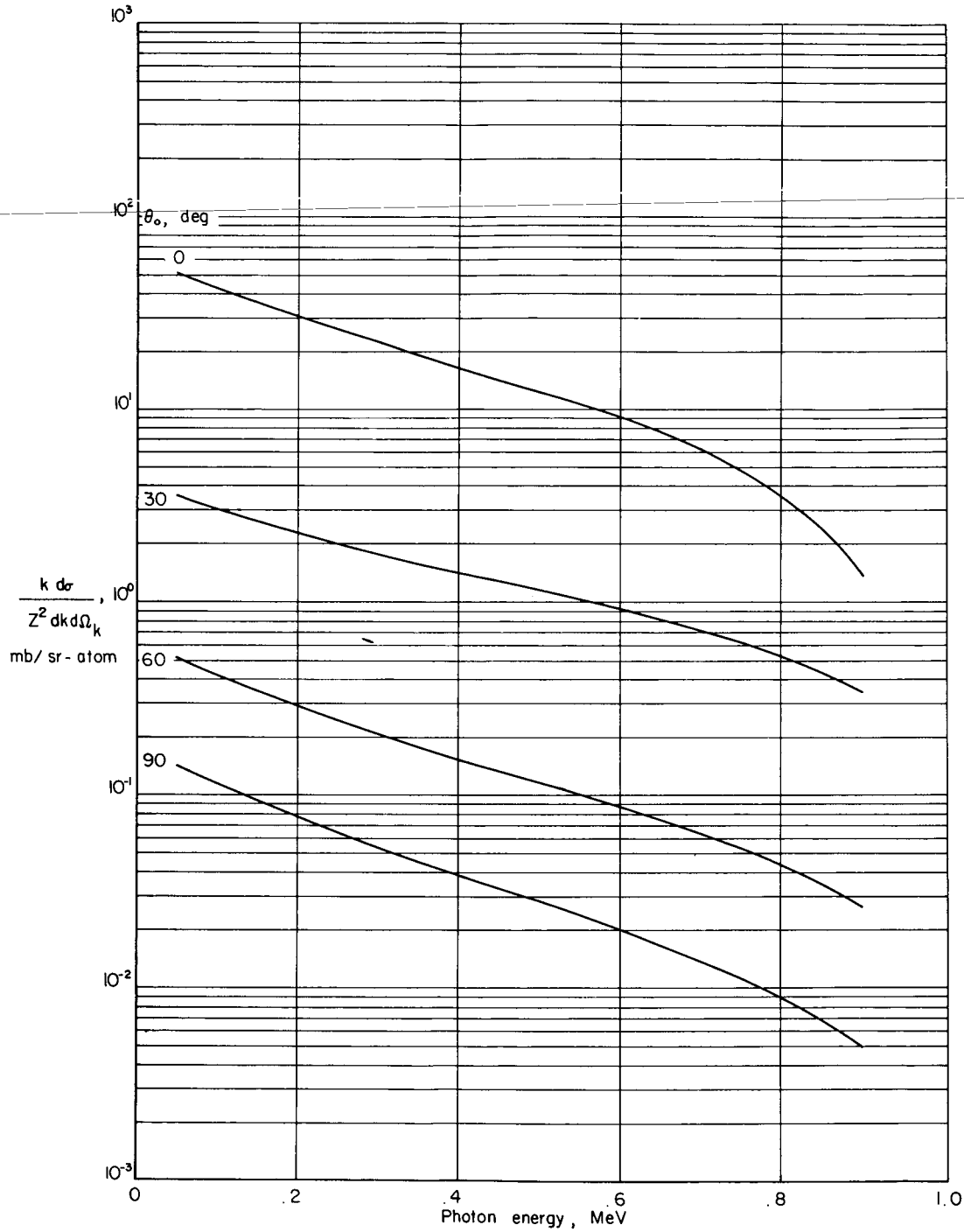

(j) Electron kinetic energy, 1.0 MeV.

Figure 2.- Continued.

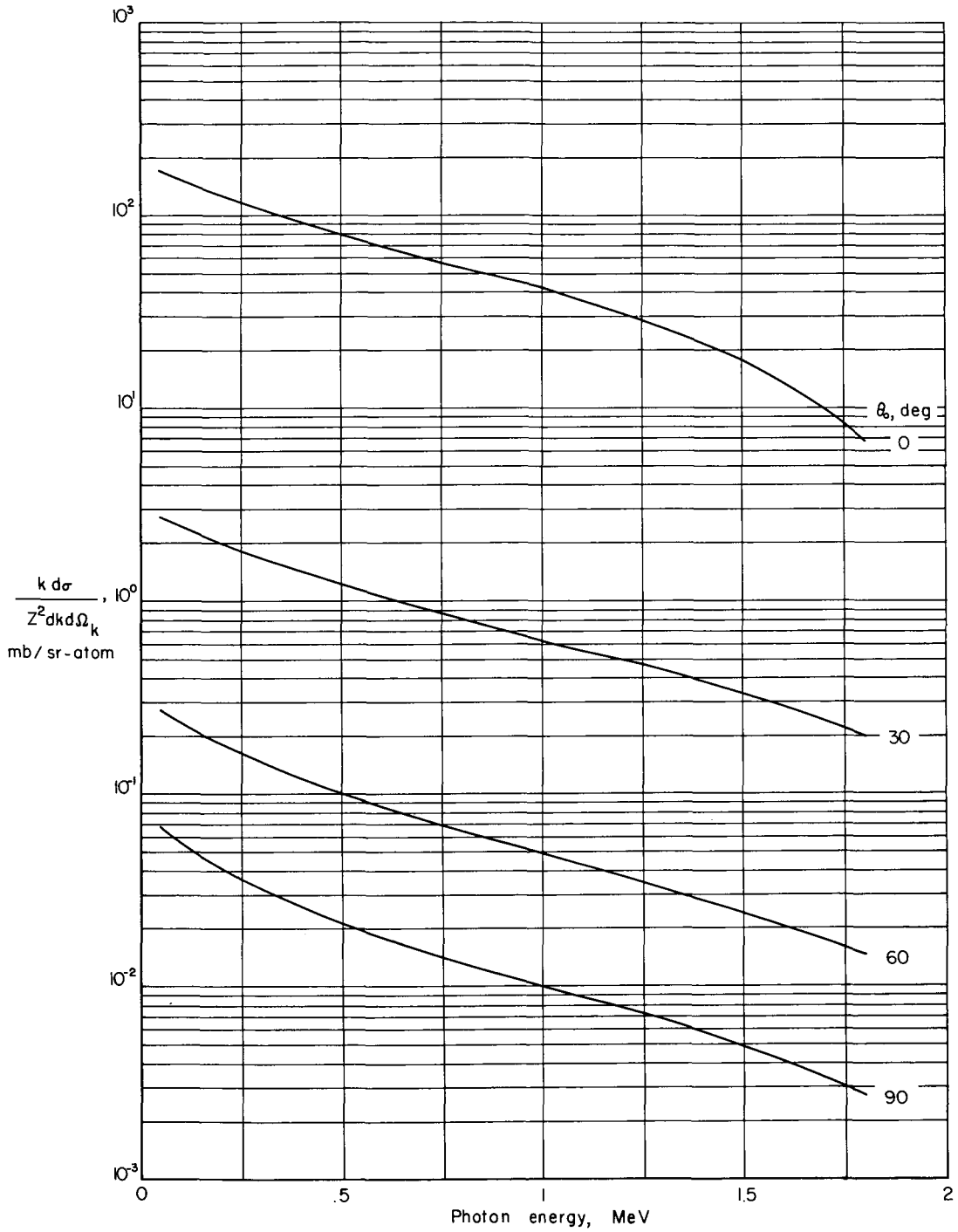

(k) Electron kinetic energy, 2.0 MeV.

Figure 2.- Continued.

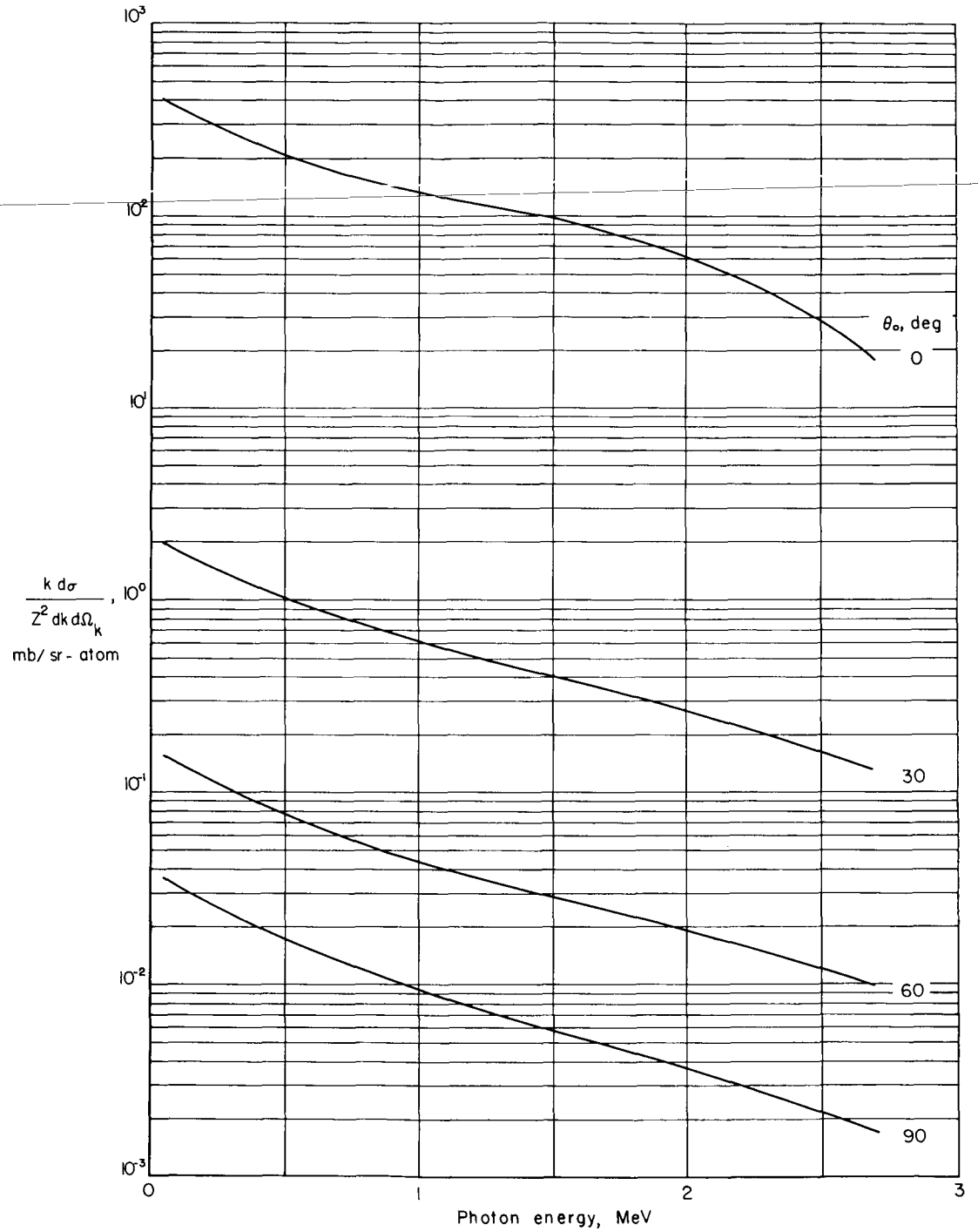

(*l*) Electron kinetic energy, 3.0 MeV.

Figure 2.- Continued.

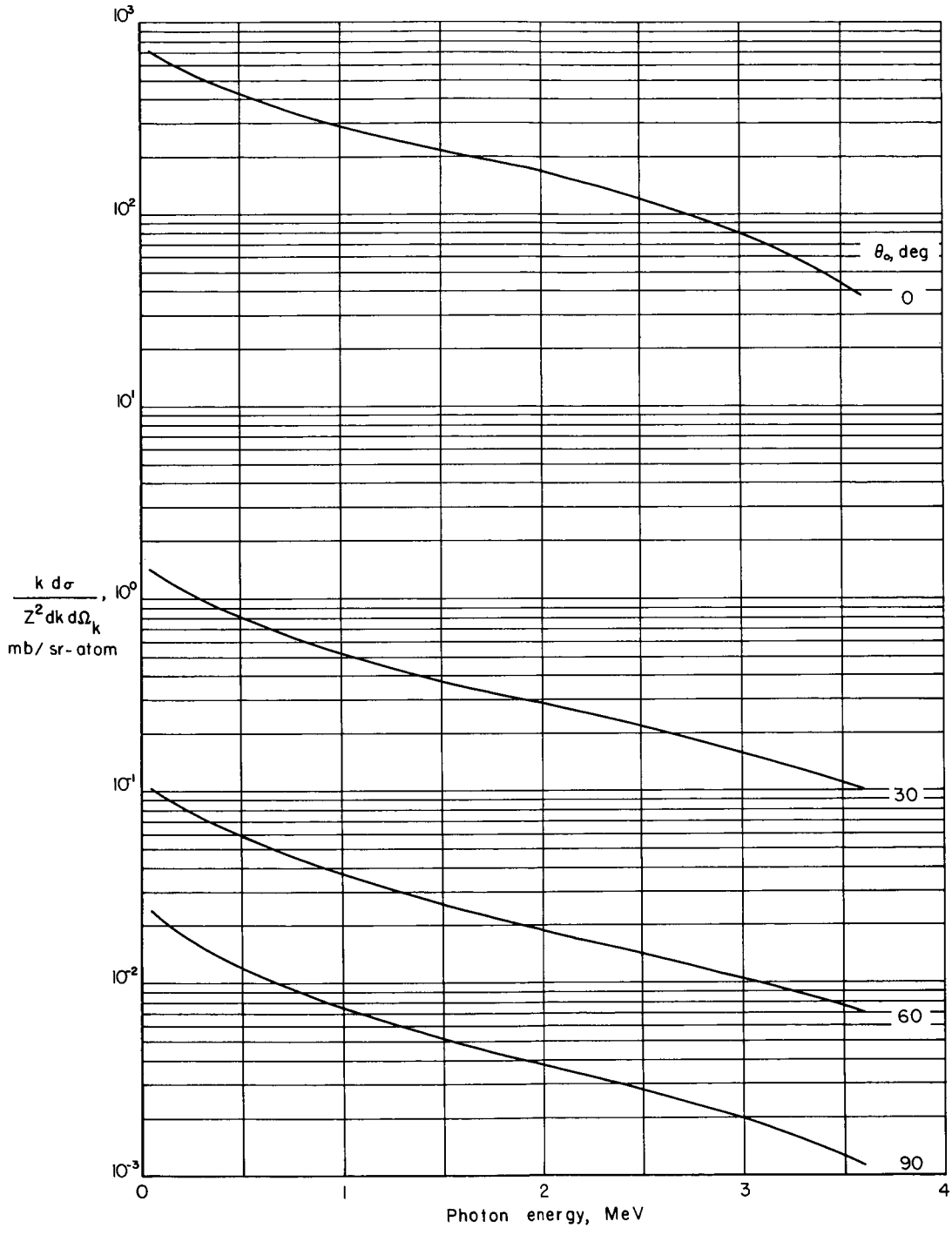

(m) Electron kinetic energy, 4.0 MeV.

Figure 2.- Continued.

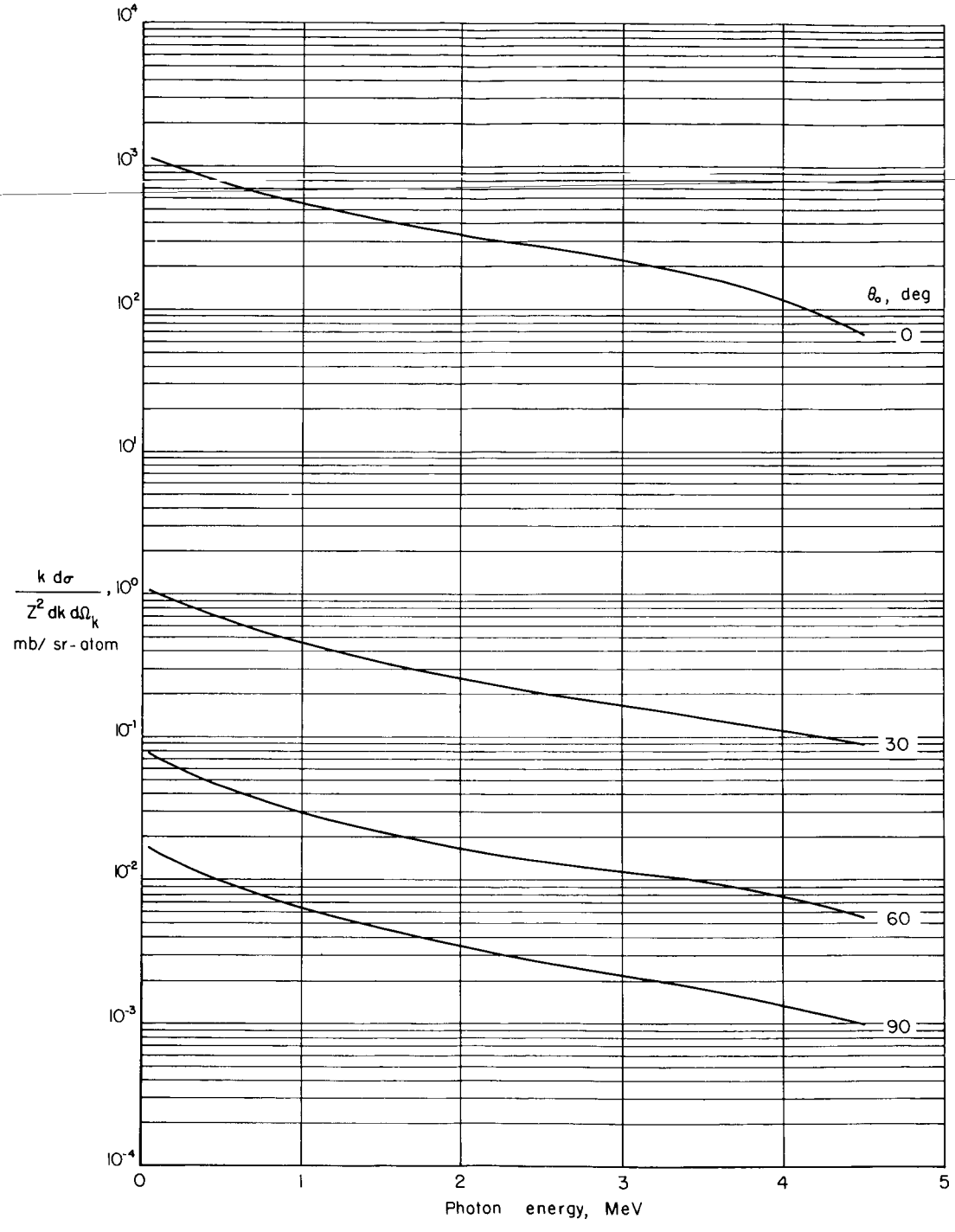

(n) Electron kinetic energy, 5.0 MeV.

Figure 2.- Continued.

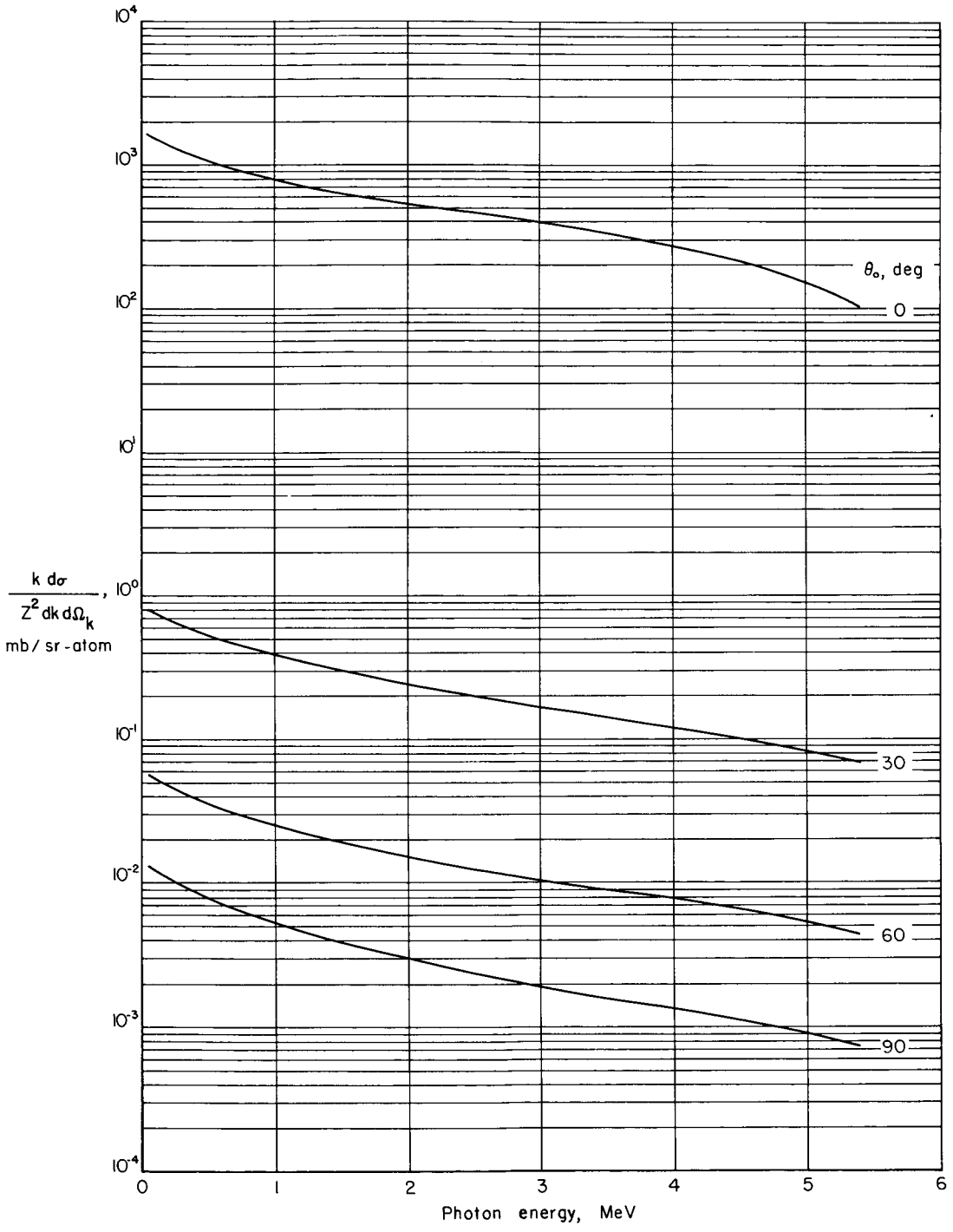

(o) Electron kinetic energy, 6.0 MeV.

Figure 2.- Continued.

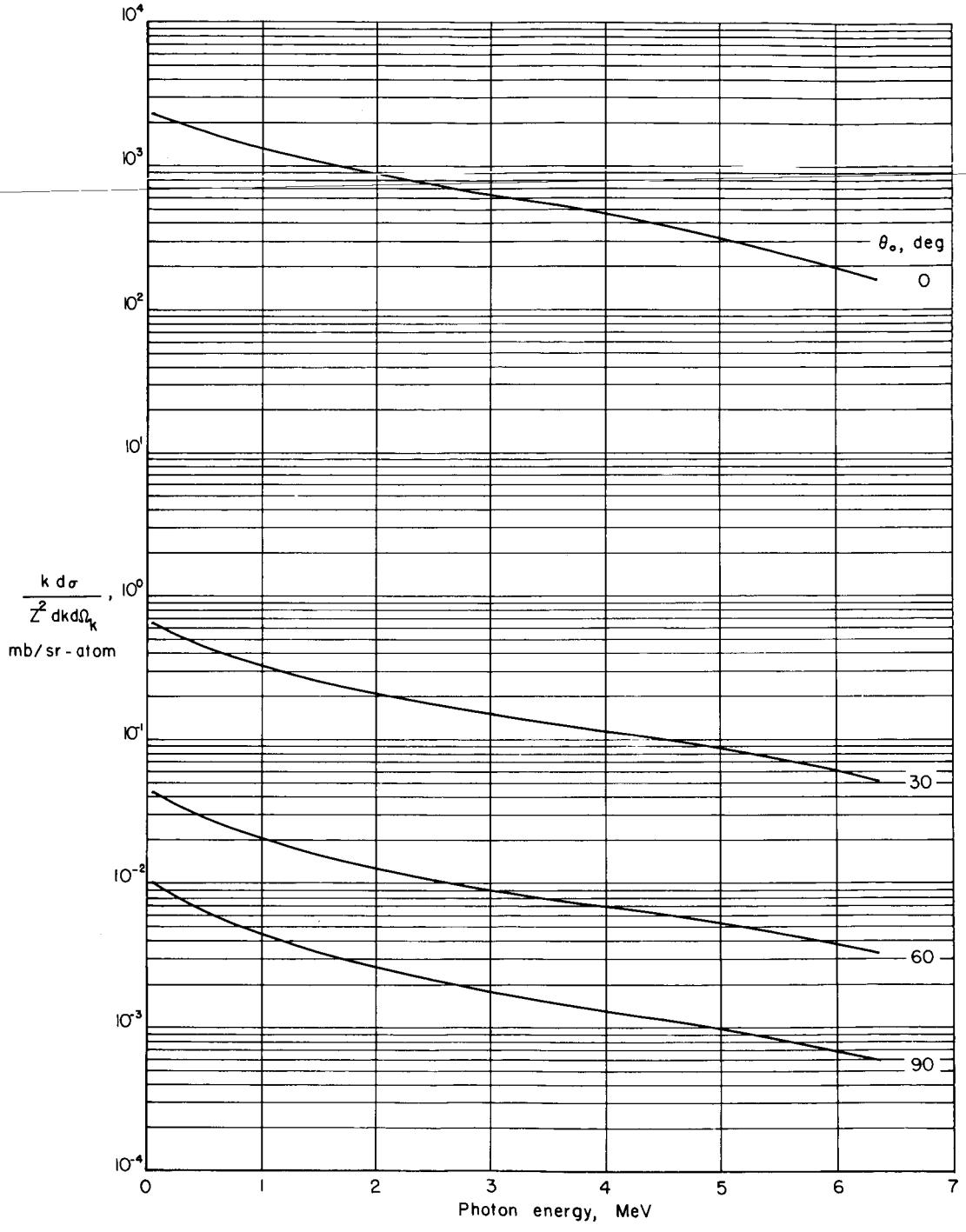

(p) Electron kinetic energy, 7.0 MeV.

Figure 2.- Concluded.

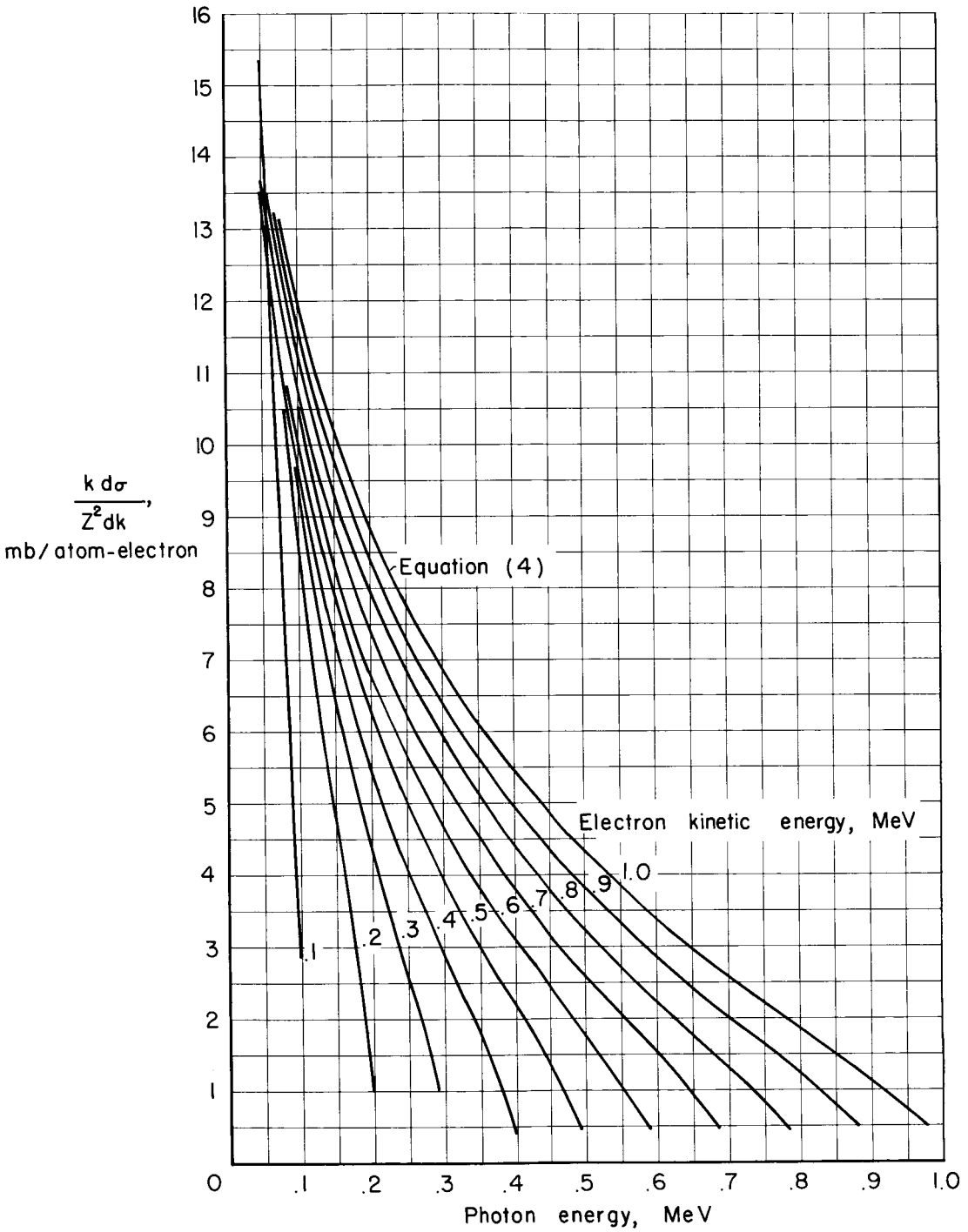

(a) Electron kinetic energy, 0.1 to 1.0 MeV.

Figure 3.- Dependence of thin-target bremsstrahlung intensity spectra on photon energy k and incident-electron kinetic energy.

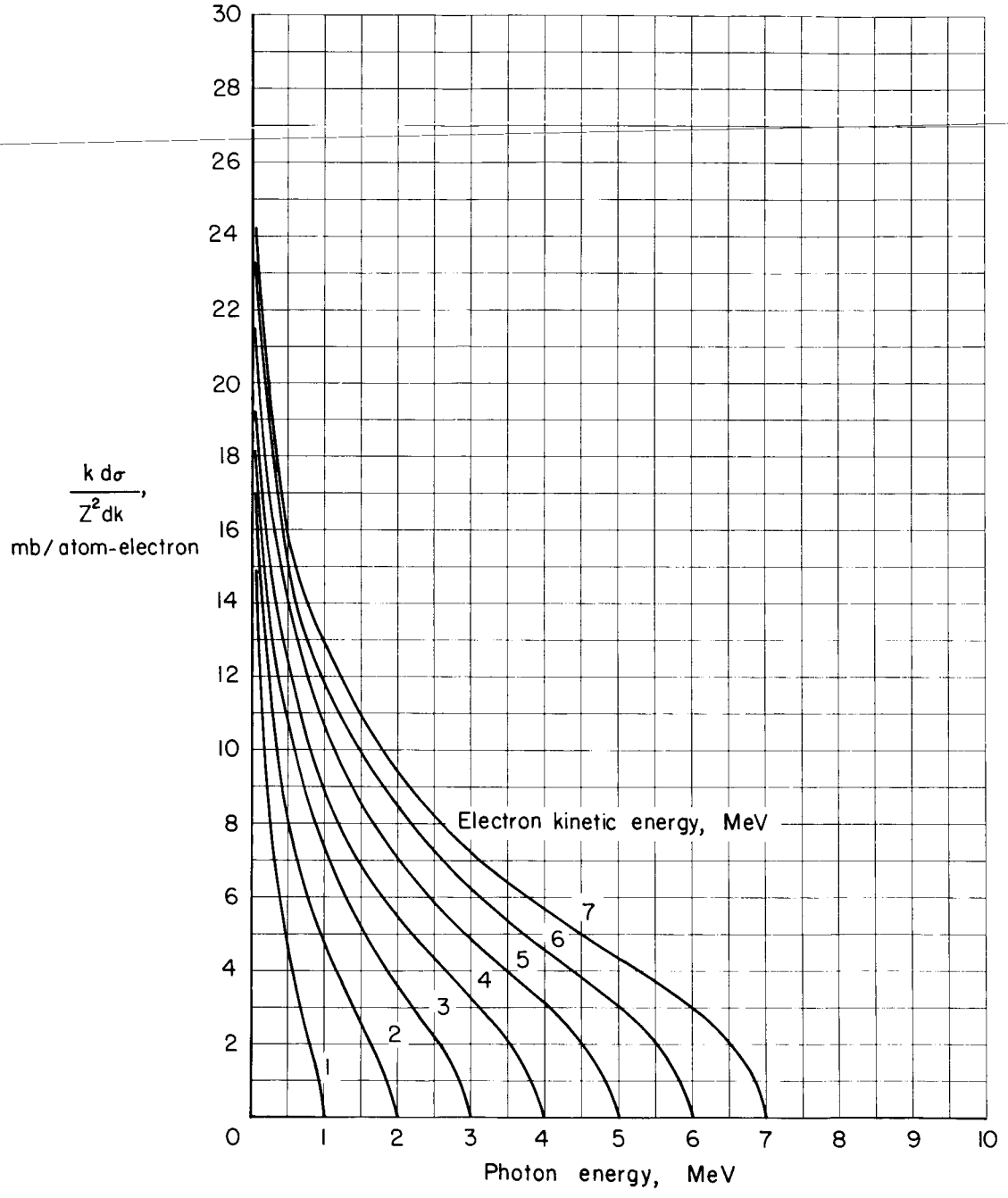

(b) Electron kinetic energy, 1.0 to 7.0 MeV.

Figure 3.- Concluded.

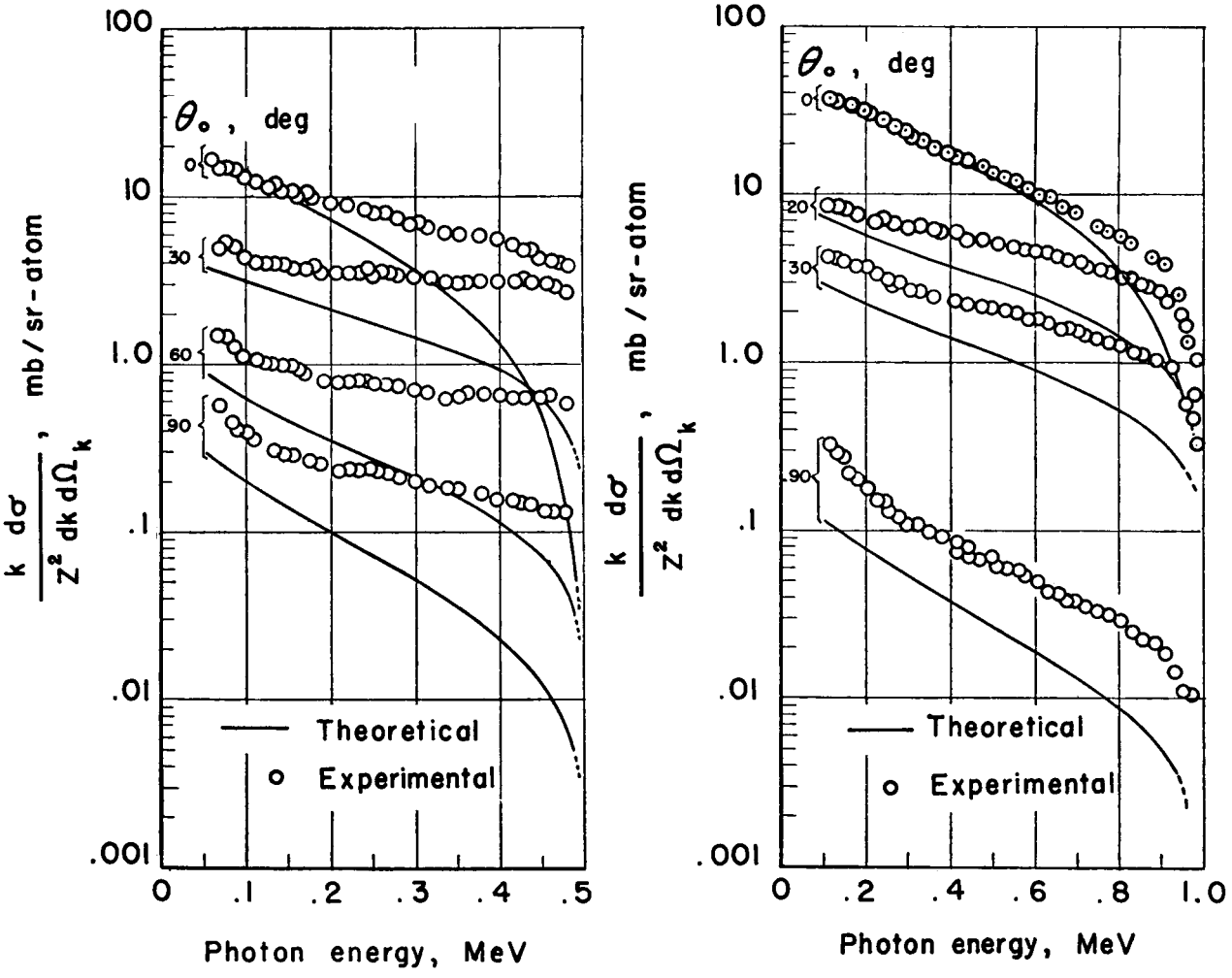

(a) Electron kinetic energy, 0.5 MeV.

(b) Electron kinetic energy, 1.0 MeV.

Figure 4.- Dependence of thin-target bremsstrahlung spectra on photon energy k and angle θ_o. Z = 79. (From ref. 2, by permission of American Institute of Physics.)

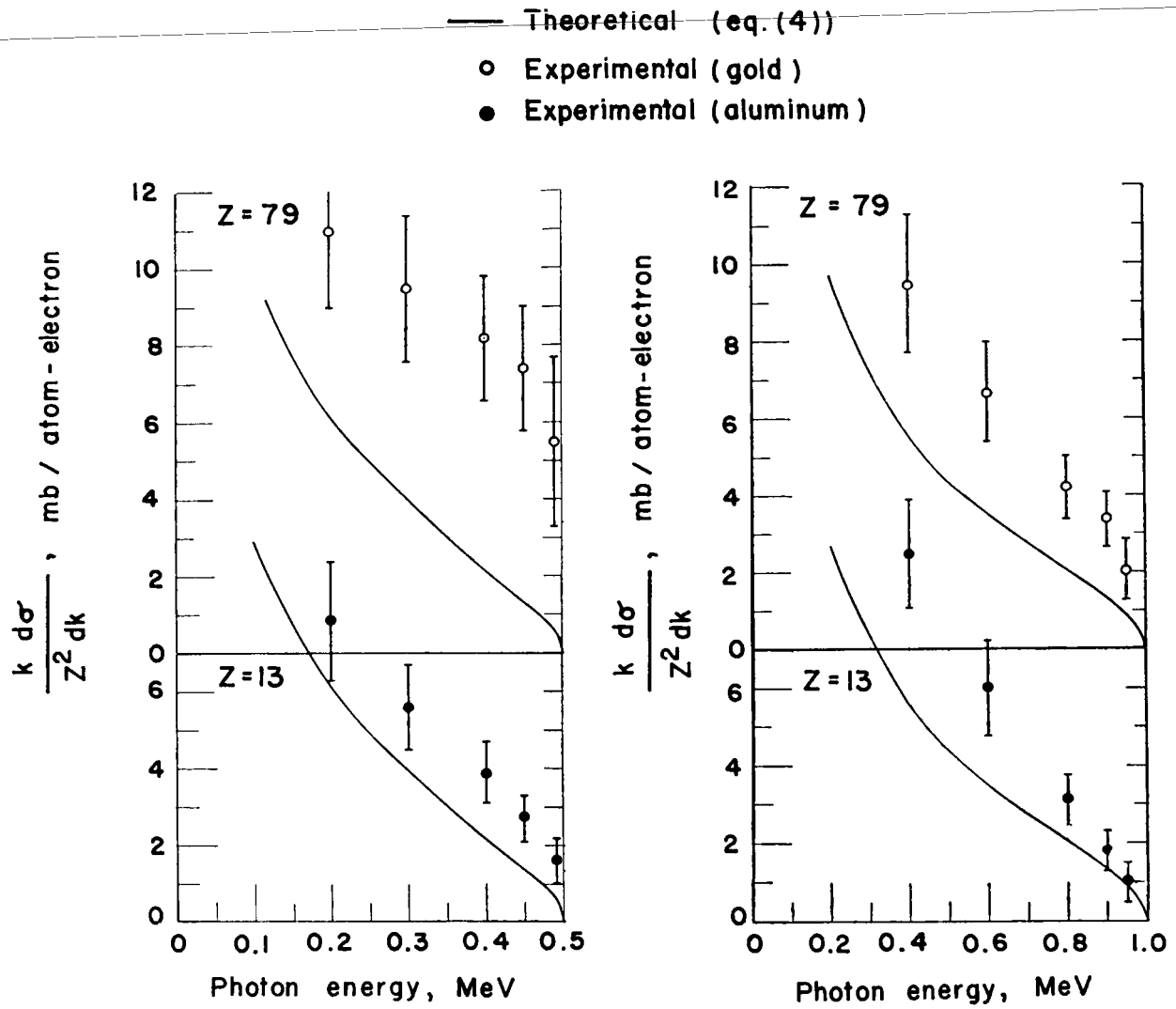

(a) Electron kinetic energy, 0.5 Mev.

(b) Electron kinetic energy, 1.0 MeV.

Figure 5.- Dependence of thin-target bremsstrahlung intensity spectra on photon energy k. (From ref. 2, by permission of American Institute of Physics.)

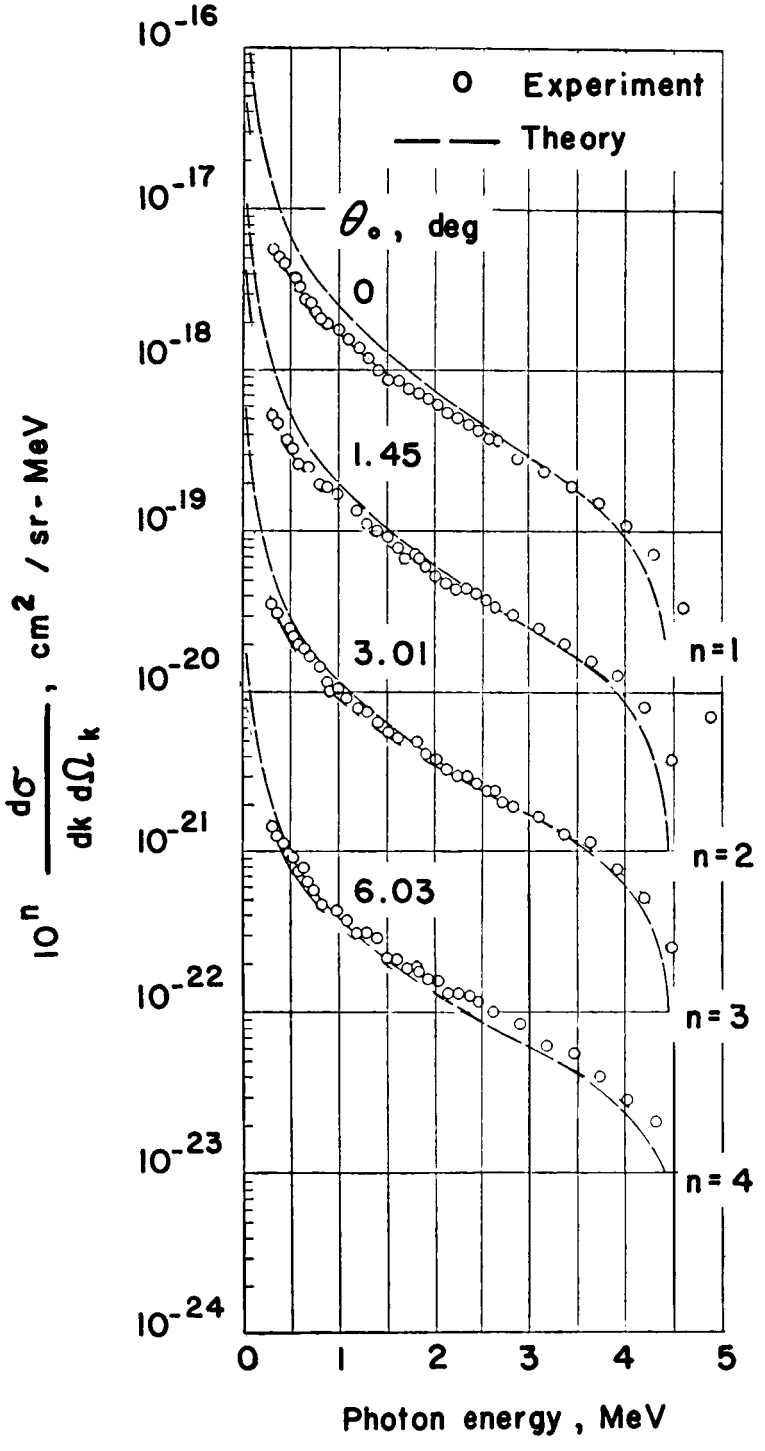

Figure 6.- Dependence of thin-target bremsstrahlung intensity spectra on photon energy k and angle θ_o for beryllium (Z = 4) and for an electron kinetic energy of 4.54 MeV. (From ref. 4, by permission of American Institute of Physics.)

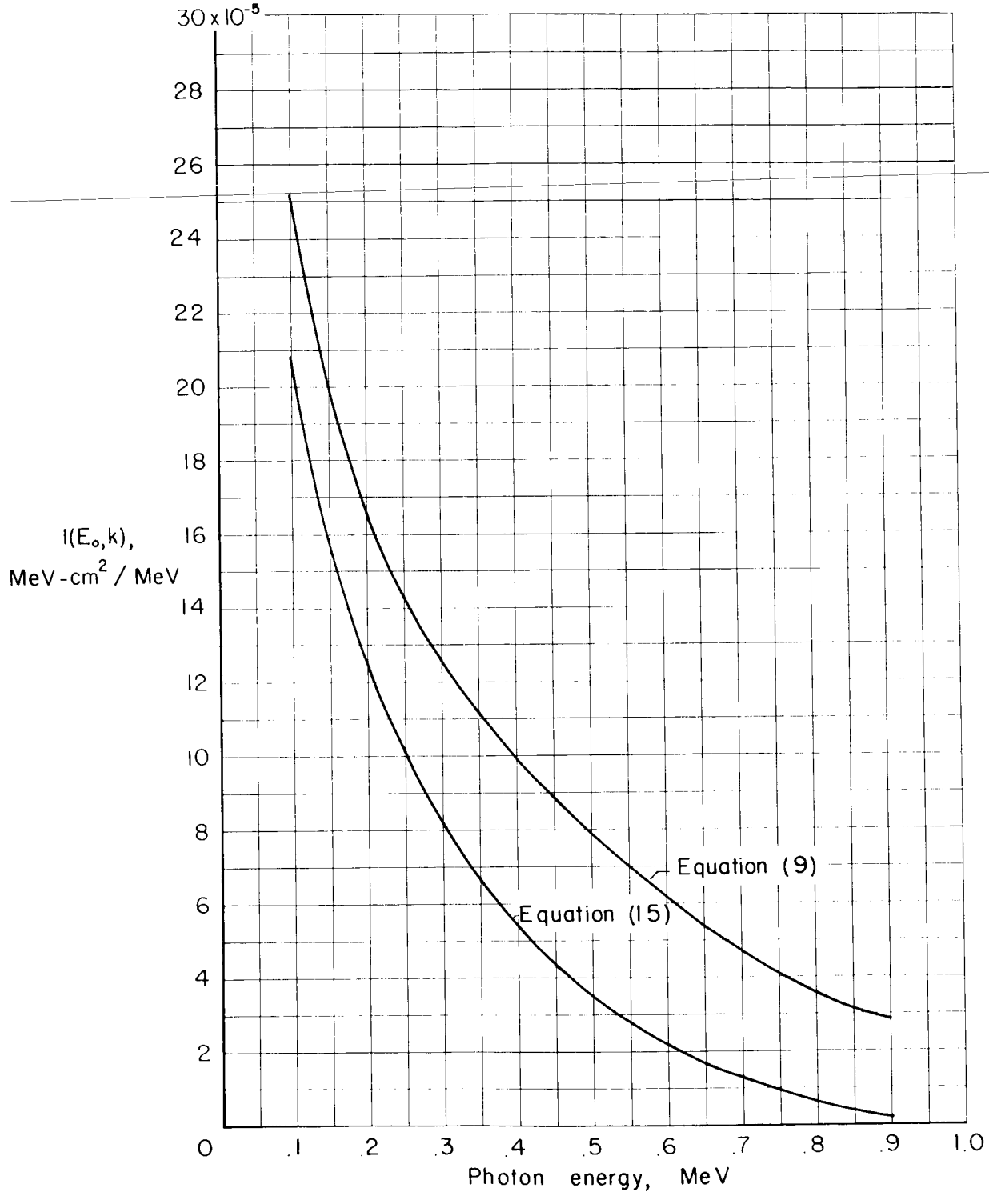

Figure 7.- Dependence of thick-target bremsstrahlung intensity spectra on photon energy k for a 1.0-MeV electron stopped in carbon.

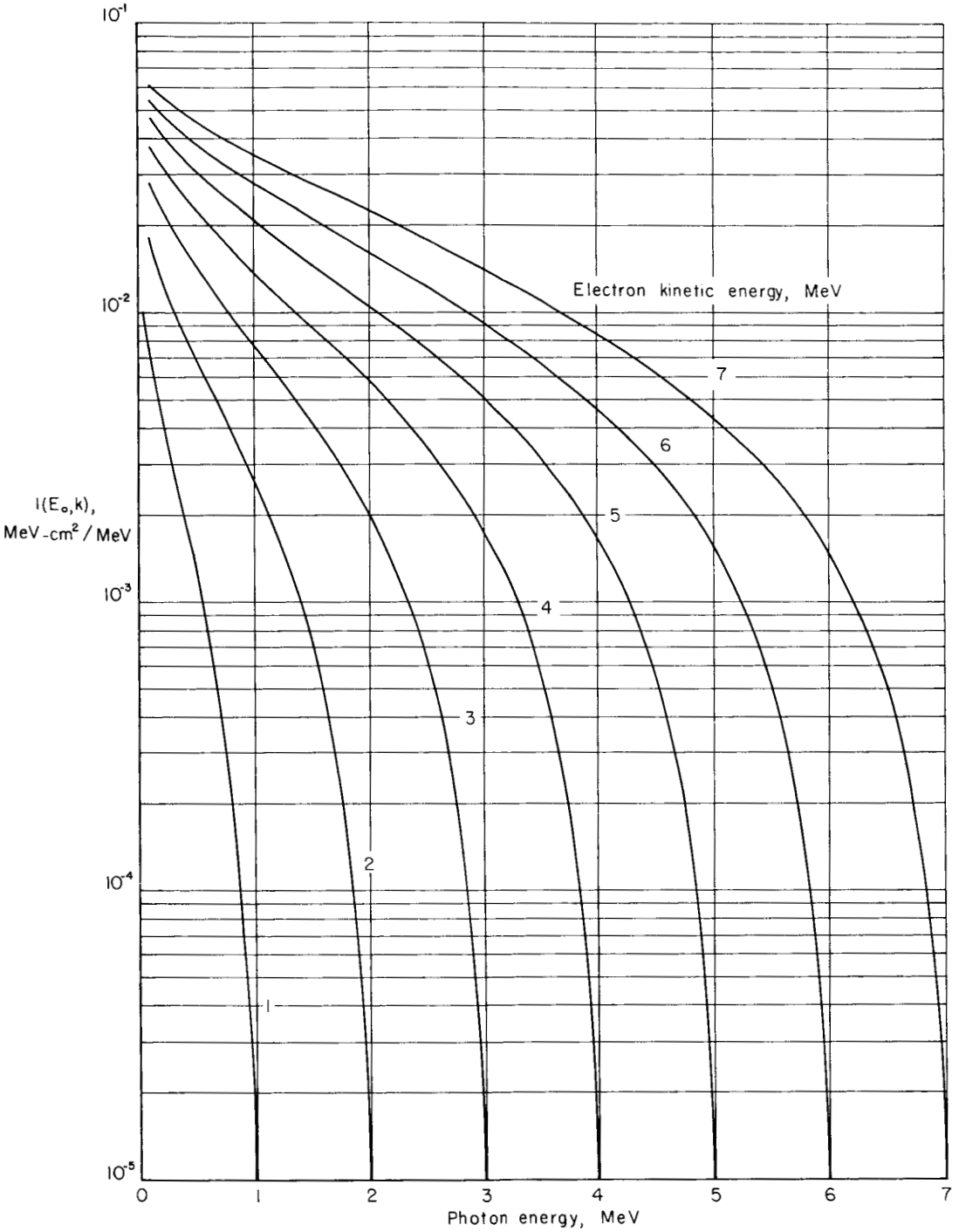

(a) Carbon.

Figure 8.- Dependence of thick-target bremsstrahlung spectra on photon energy k and incident-electron kinetic energy.

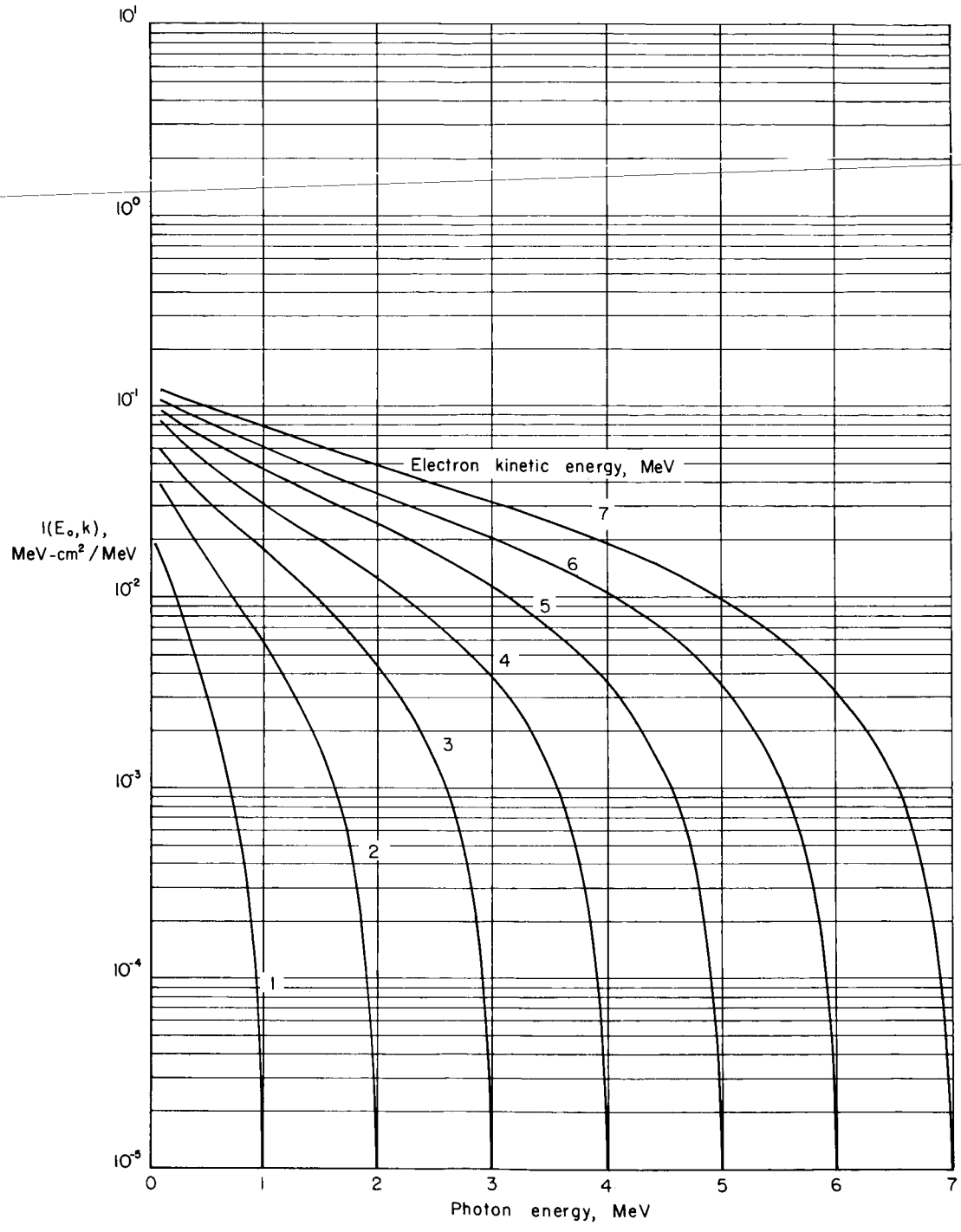

(b) Aluminum.

Figure 8.- Continued.

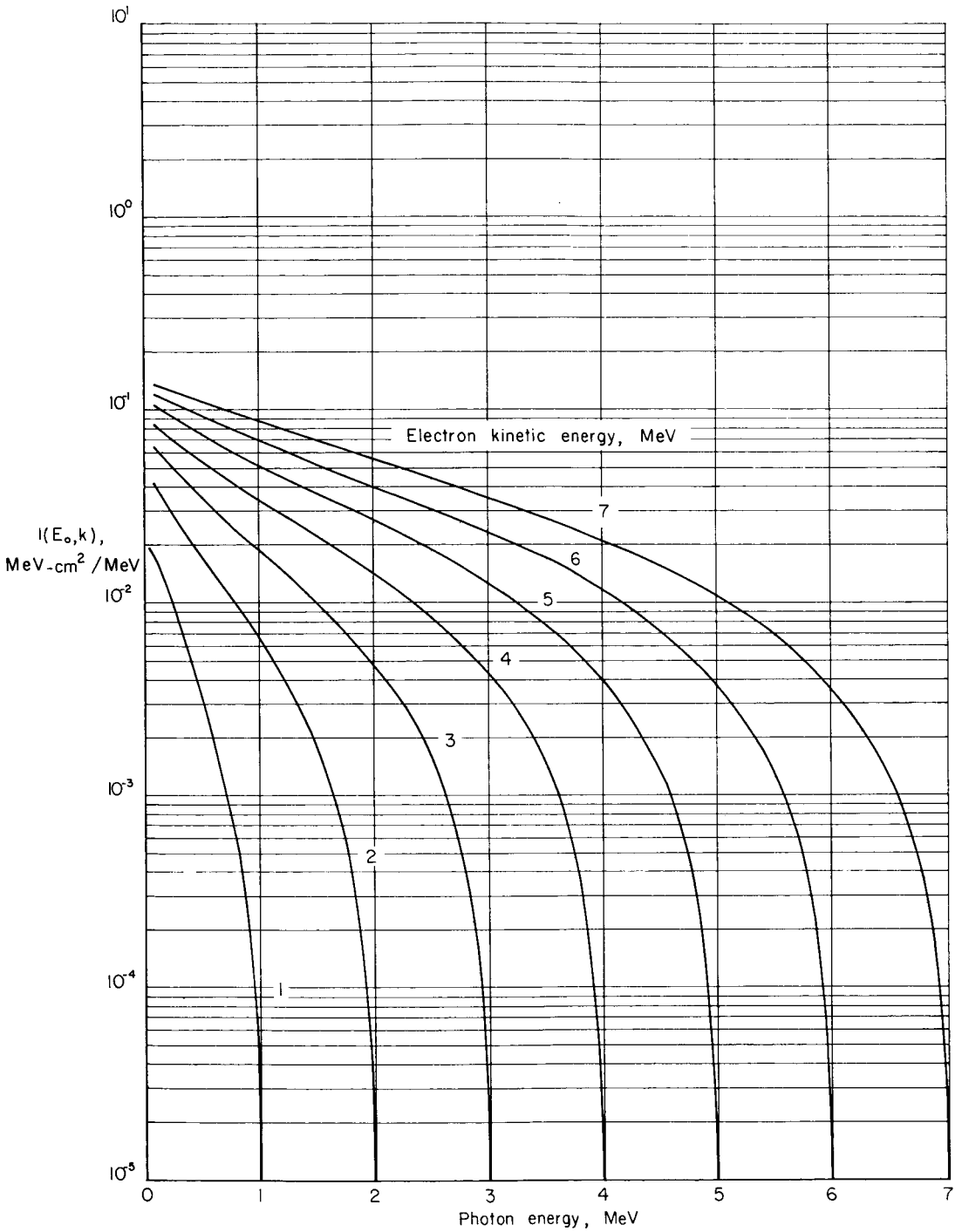

(c) Silicon.

Figure 8.- Continued.

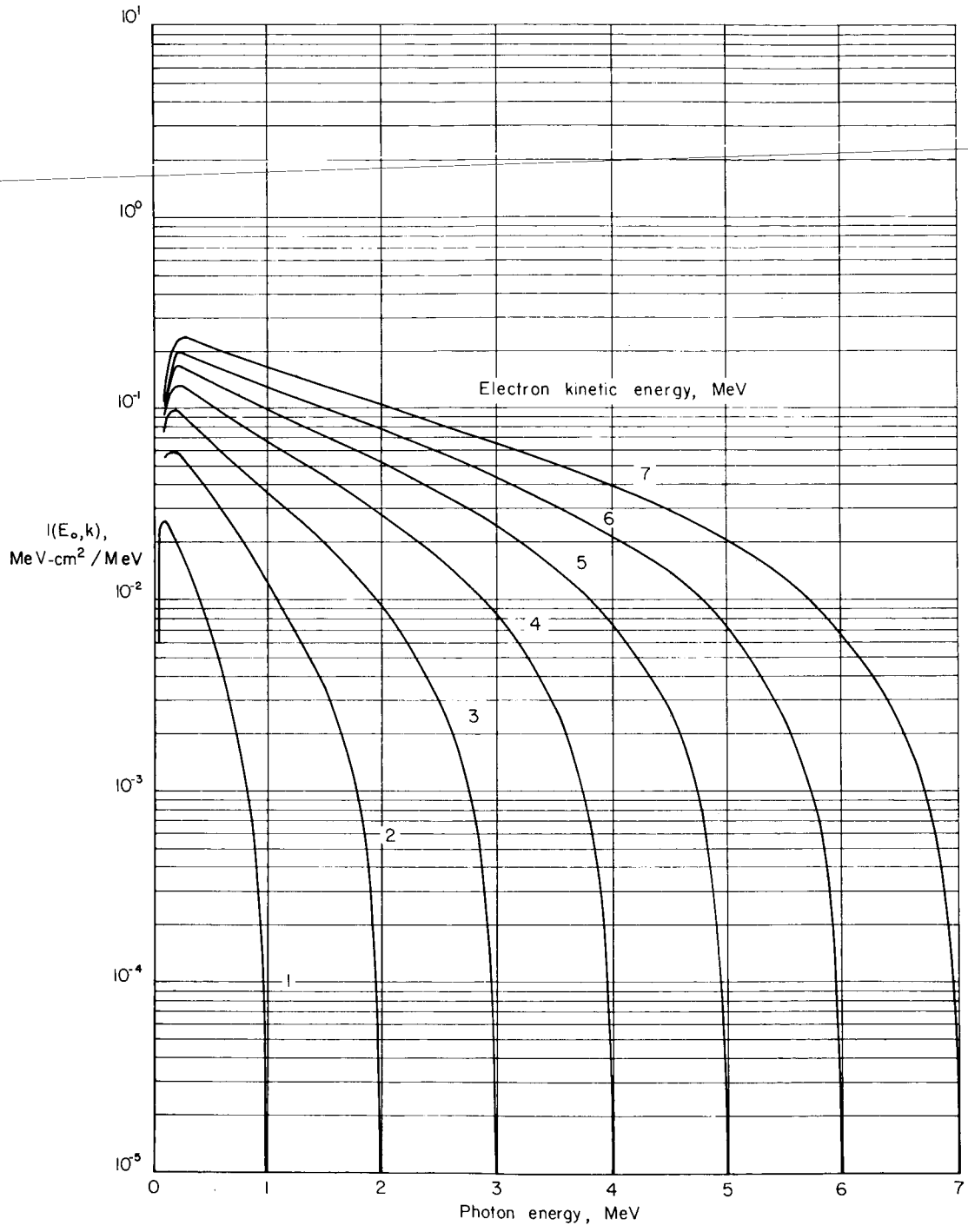

(d) Iron.

Figure 8.- Concluded.

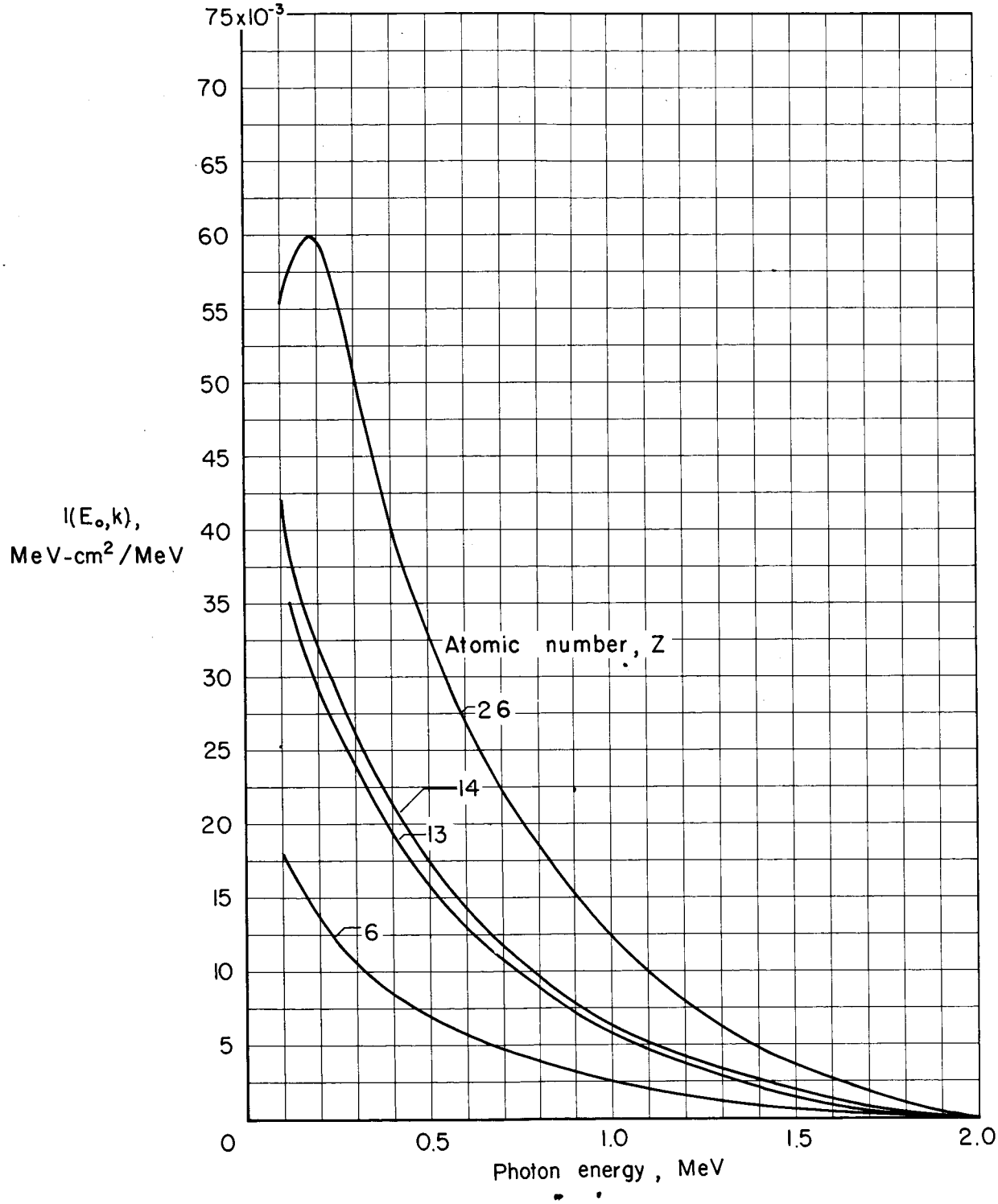

Figure 9.- Dependence of thick-target bremsstrahlung spectra on photon energy k and atomic number Z for incident electron with kinetic energy of 2 MeV.

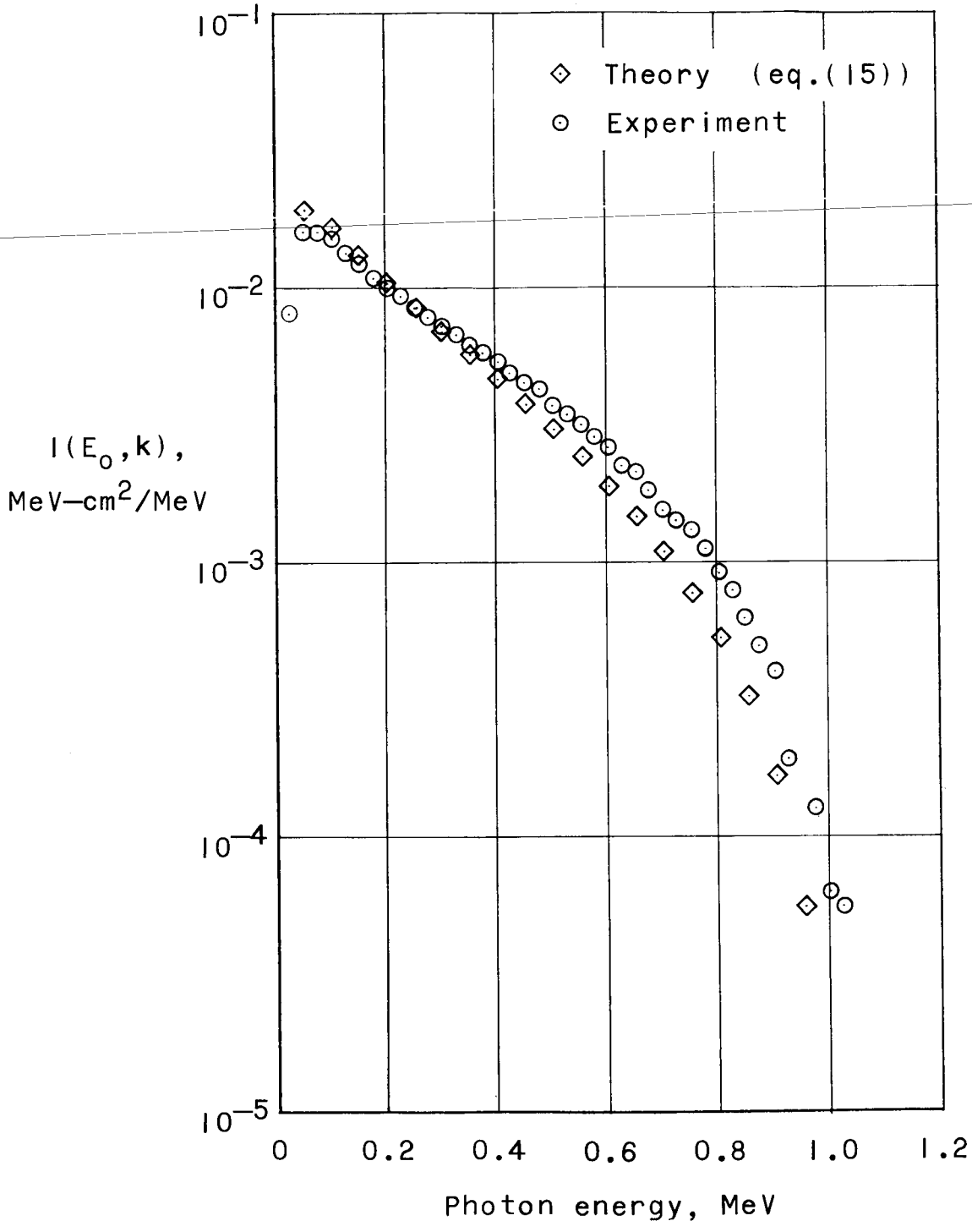

Figure 10.- Comparison of straight-through theory (eq. (15)) and experiment for 1.0-MeV electrons stopped in aluminum. (Experimental data supplied by Ling-Temco-Vought Research Center under NASA Contract No. NASw-647.)

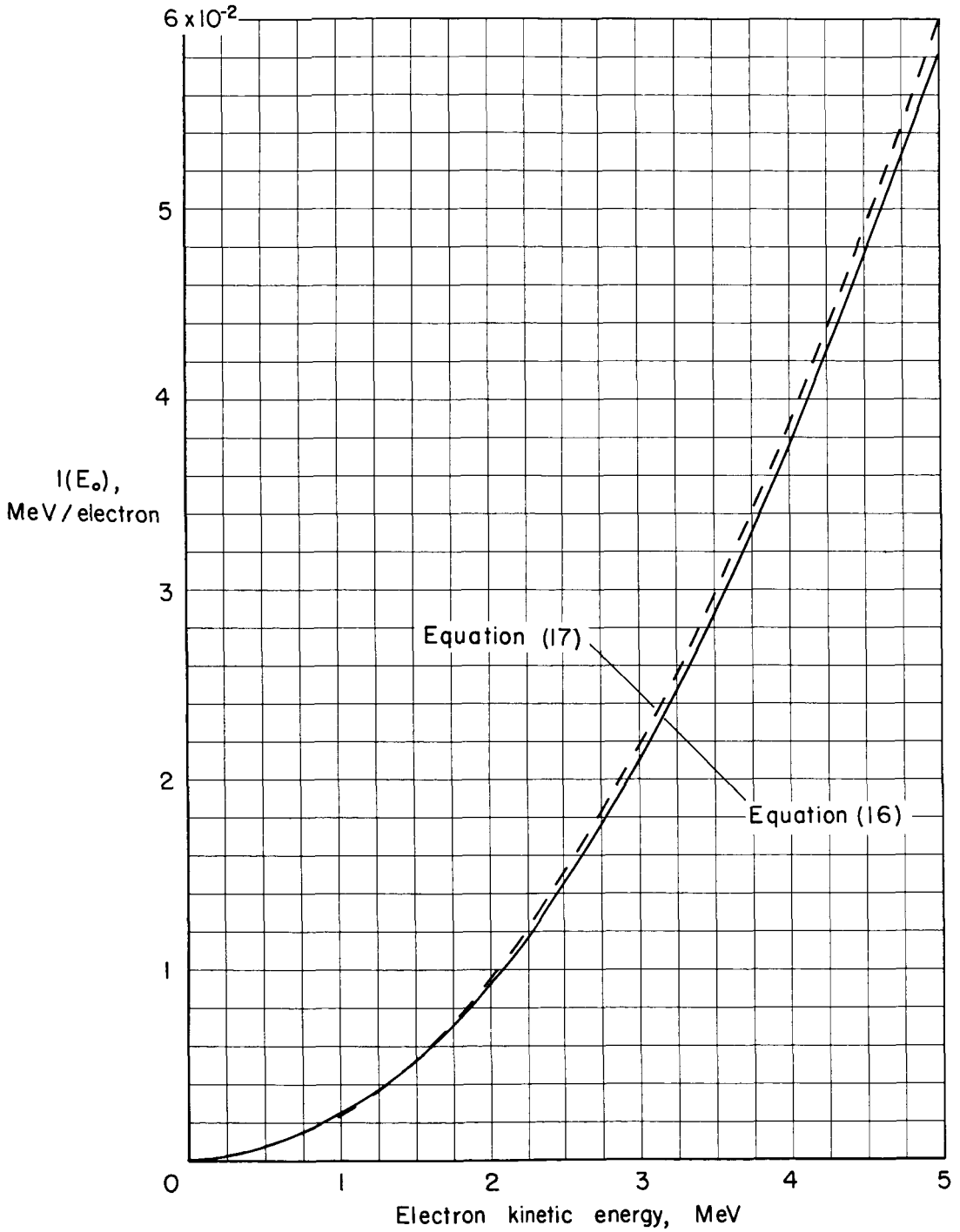

Figure 11.- Comparison of total bremsstrahlung energy predicted by semi-empirical relation (dashed curve) and straight-through theory (solid curve) when an electron is stopped in a carbon target (Z = 6) as a function of the electron kinetic energy.

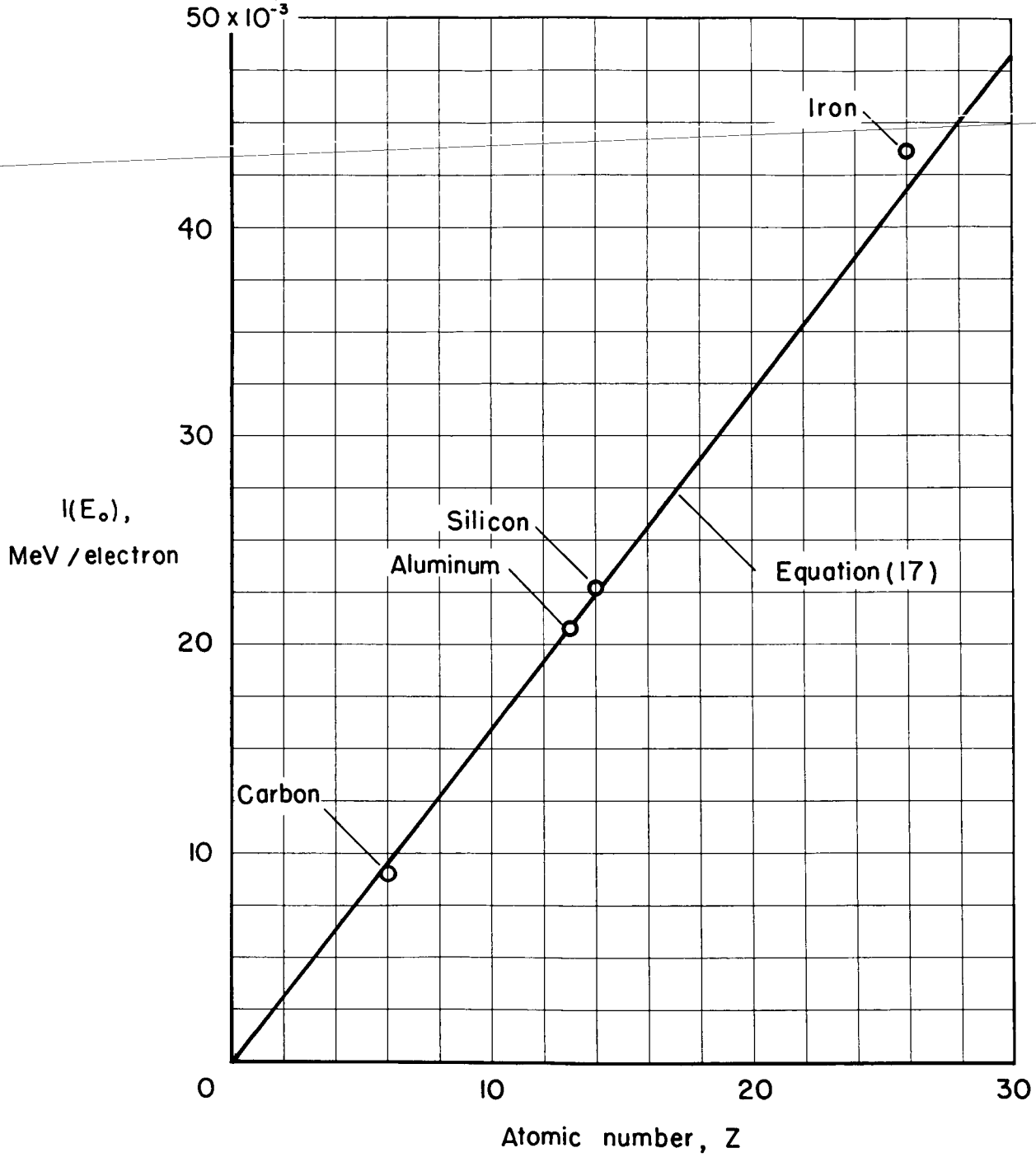

Figure 12.- Comparison of total bremsstrahlung energy predicted by semi-empirical relation (solid curve) and straight-through theory (open circles) when a 2.0-MeV electron is stopped in thick targets of carbon, aluminum, silicon, and iron as a function of atomic number Z.

NASA-Langley, 1965 L-3675